Seismic sequences and swarms in the Latium-Abruzzo-Molise Apennines (central Italy): new observations and analysis from a dense monitoring of the recent activity

A. Frepoli, G.B. Cimini, P. De Gori, G. De Luca, A. Marchetti, S. Monna, C. Montuori, N.M. Pagliuca.

Istituto Nazionale di Geofisica e Vulcanologia,via di Vigna Murata, 605 -00143 Rome, Italy

Abstract

We present a detailed analysis of the seismic activity in the central Apennines based on a high quality seismogram data set collected from two temporary and three permanent networks. This integrated network recorded, between January 2009 and December 2013, a total of 7011 local earthquakes (6270 selected for this study), with local magnitudes M_L ranging from 0.4 to 4.7. Hypocentres were located by using a reference1D crustal velocity model determined with a genetic algorithm. The majority of the hypocenters are located beneath the axis of the Apenninic belt, while the rest are found along the peri-Tyrrhenian margin. Hypocentral depth distribution extends to a depth of 31 km with a pronounced peak between 8 and 12 km. Both low-to-moderate magnitude seismic sequences and diffuse swarm-like seismicity was observed. There were two major seismic swarms and a seismic sequence, which included the Marsica-Sora M_L 4.7 main shock. A total of 468 fault plane solutions were derived from *P*-wave polarities. This new data set more than quadruples the number of focal mechanisms that was previously available for regional stress field analysis in the study region. The majority of the fault plane solutions in the central Apennines show predominantly normal fault movements, with T-axis trends oriented NE-SW. Focal mechanisms calculated in this study confirm that this area is in extension. For the seismic swarms-sequence in the Marsica-Sora area we also derived the azimuth and plunge of the principal stress axes by inverting fault plane solutions.

We find a few right-lateral strike-slip focal mechanisms that possibly identify the prolongation of the strike-slip kinematics in the Gargano-Apulia foreland to the west, and mark the passage to the NW-SE striking normal faults of the inner Apenninic belt. The seismicity and stress distribution we observe might be consistent with a fragmented tectonic scenario in which faults with small dimensions release seismic energy in a diffused way.

1. Introduction

The Apenninic belt is the result of the convergence between the Eurasian and African plates (Anderson and Jackson, 1987; Doglioni, 1993; Serri *et al*., 1993; Jolivet *et al*., 1998), which is now taking place at a rate of ~ 10 mm/yr along a ~ NS direction (De Mets *et al*., 1994). NE-trending extension in the central Apennines, which began in the Pliocene (Patacca and Scandone, 1989; Patacca *et al*., 1990), produces a broad and complex system of NW-SE trending normal faults with related large intermountain extensional basins (Galadini and Galli, 2000; Cavinato *et al*., 2002; Montone *et al*., 2004). In the central Apennines the fault systems and individual faults are organized into two principal sets that run almost parallel to the belt axis, the eastern and western normal fault systems (Figure 1) (Galadini and Galli, 2000; Valensise and Pantosti, 2001; Boncio *et al*., 2004; Basili *et al*., 2008). Several Quaternary normal faults show a clear signature at the surface and paleoseismological evidence of Holocene surface faulting earthquakes (Pantosti *et al*., 1996; Galadini and Galli, 2000; D'Addezio *et al*., 2001; Roberts and Michetti, 2004; Papanikolaou *et al*., 2005), but these sub-surface data poorly constrain the deep geometry of most of these faults. At present the Apennines thrust and fold belt is accommodated by a NE-trending extension with a rate of about 3-4 mm/yr (D'Agostino *et al*., 2008; D'Agostino *et al*., 2014; Palano, 2015). The northern Apennines are almost continuously releasing seismicity, while the central Apennines have been silent during the past decades, with only few and sparse events occurring around the main faults (Bagh *et al*., 2007; De Luca *et al*., 2009; Romano *et al*., 2013).

Historically, the study region has been affected by many strong earthquakes, some of them very destructive and with effects even in the greater Rome area. Several urban centres with more than 10,000 inhabitants are very close to the complex system of active faults that can be up to 20-30 km long (Figure 1). The central and southern Apennines have the highest seismic potential in the Italian region, with recurrence times for $M_w \geq 6.5$ events between 60 and 140 years (Jenny *et al*., 2006).

Figure 1 shows the greatest earthquakes that have occurred in this area, the main ones being the 1456 Molise-Campania event, possibly the largest earthquake that has ever occurred in peninsular Italy (M_w ~ 6.5-7.0), and the 1915 Marsica event (M_w 6.7, number 7 in Figure 1; Amoruso *et al*., 1998). Both earthquakes caused effects of the XI degree on the Mercalli-Cancani-Sieberg scale (MCS). The M_w 5.9 May 7, 1984 Val Comino earthquake is the strongest recent instrumentally recorded event in our study area. The main shock was followed by intense seismic activity, including the large M_w 5.5 aftershock on May 11 (Del Pezzo *et al*., 1985). The focal mechanisms of these two events are quite similar, mostly extensional with the extensional axis (T) oriented at about N60°E (Westaway *et al*., 1989; Pace *et al*., 2002), and therefore confirm an ongoing NE-SW extension in the region. Finally, on February 20, 2008, in the Cassino area, an M_w 4.2 earthquake occurred on a NW-SE normal fault at 10 km hypocentral depth (ISIDe Working Group, 2010).

The study area (Figure 1) borders regions that have been recently affected by destructive events such as the M_w 5.8 Molise (October 31, 2002), the M_w 6.1 L'Aquila (April 6, 2009), the M_w 6.0 Amatrice (August 24, 2016), and the M_w 6.5 Norcia (October 30, 2016). During the five-years of our observing period, we recorded both low-to-moderate magnitude seismic sequences and diffuse swarm-like seismicity. These clusters were spatially concentrated within areas of about 50 km^2 or less.

Seismic swarms are a localized surge of earthquakes striking in a relatively short time (days, weeks or months). Typically, they are not triggered by stress changes caused by a dominant earthquake and may include several earthquakes of similar magnitude. Differently from seismic sequences the largest events do not necessarily occur early in the seismic crisis, and do not follow the Omori law. Swarm activity is generally associated to processes that are not directly observable, such as pore-pressure changes due to the diffusion of fluids (Hainzl *et al*., 2012 and references therein). On the other hand, seismic sequences are characterized by a main shock that usually occurs at the beginning of the crisis, followed by a series of aftershocks that satisfies the Omori law distribution. Seismic swarms have been detected also in other sectors of the Apennines extensional belt, such as the Pollino range (Passarelli *et al*., 2015) and the area of the Gubbio basin (Marzorati *et al*., 2014). Also, tectonic earthquake swarms have been recorded in several areas in Europe: Tjörnes Fracture Zone – North Iceland (Hensch *et al*., 2008), Vogtland/West Bohemia –Germany/Czech Republic border (Hainzl *et al*., 2012), and in southern California (Vidale and Shearer, 2006). The suggested triggering models for swarms are pore-pressure diffusion (West Bohemia) and aseismic creep (California). Deep fluids, upwelling from the delaminating continental lithosphere, have been considered to explain seismicity clustering in the upper crust and lubrication of faults during swarms and large earthquakes (Marzorati *et al*., 2014).

The main objective of this work is to provide, thanks to a dense seismic network, a detailed description of the pattern of seismicity that occurred during five years in this part of the central Apennines. It was possible to record and locate a large amount of otherwise undetected seismicity, calculate a considerable number of well-constrained focal mechanisms, and infer the geometry of the active faults involved. Furthermore, we performed a detailed mapping of the active stress field retrieved from focal mechanism inversion within the Marsica-Sora area (hereinafter MSA), where most of the studied seismicity was recorded.

2. Seismic networks

The study region extends in latitude from 41.1N to 42.3N, and in longitude from 12.6E to 14.8E (Figure 1). It includes the Velino-Sirente Mts. and the Maiella Massif to the north, the Tyrrhenian coast to the south-west and the Volturno Plain to the south, and the Frentani/Matese Mts. to the east. It also includes a ~150 km long portion of the central Apenninic belt and the peri-Tyrrhenian volcanic complex of Alban Hills and Roccamonfina.
The data presented in this study were recorded by both permanent and temporary seismic networks (Figure 2). Italian permanent seismic networks, both national and regional, have been significantly extended in the last two decades through installation of new three component, mostly broadband, stations. The additional deployment of two temporary networks further improved the detection and location of the seismicity in the central Apennines.
The first temporary networks (up to 4 stations, Moretti *et al*., 2011) was part of a pilot study that took place in the MSA during October 2009 - January 2010 (Table 1a). This study was prompted by the occurrence of a seismic swarm with maximum M_L 3.6, that generated worry in the local population since it took place a few months after the occurrence of the destructive nearby L'Aquila earthquake (April 2009). The second network (up to 17 stations), which covered the whole study area in the period November 2011 – December 2013, was a temporary deployment within the SLAM (Seismicity of Lazio, Abruzzo and Molise region) project (Cimini *et al*., 2013). During this second experiment three deployment sites of the pilot study were re-occupied. The 17 temporary stations were deployed in 31 different sites to improve the detection of small earthquakes (Table 1b). The permanent seismic networks operating in the area were: the Italian National Seismic Network (RSN) of the Istituto Nazionale di Geofisica e Vulcanologia (INGV) with 48 stations, the Abruzzo Regional Seismic Network (RSA; De Luca *et al*., 2009) with 28 stations, and the Molise Regional Seismic Network (RSM) with 5 stations. Furthermore, digital data recorded by three seismic stations of the IESN (Italian Earthquake Seismic Network) of southern Lazio and those of a temporary INGV station (February-April 2013) installed at Arpino (Sora area) were also available. In total the seismic analysis performed in this study was based on 98 stations. Table 1a and Table 1b shows the station equipment used in the two temporary arrays. Almost all stations were installed on hard rock formations or concrete floor on rock formation. Site selection was performed by analyzing the Power Spectral Density (PSD) of ground acceleration samples (Cimini *et al*., 2006; Trnkoczy *et al*., 2012).

3. Data analysis and results

3.1 1D velocity model

To accurately relocate seismicity we calculated, by using a global optimization procedure, a reliable 1D model for the study area. The 1D V_p velocity model (Figure 3) has been computed by the application of a genetic algorithm (Holland, 1975; Sambridge and Gallagher, 1993). We use a constant value of 1.84 for V_p/V_s determined with the Wadati method (Chatelain, 1978). Genetic algorithms (GA) are optimization methods that are widely used to solve highly non linear inverse problems, such as earthquake location and 1D velocity model determination (Sambridge and Gallagher, 1993; Bagh *et al*., 2007). The GA sampled a large number of possible velocity models. Starting from each model, we located all the seismic events by using the Hypoellipse code (Lahr, 1989) and we evaluated a global unweighted RMS that represents the cost function (or the fitness) of the optimization problem being solved. The goal of a GA is to progressively modify the velocity model to find an optimal solution that (hopefully) is the absolute minimum of the cost function. After several trials, we chose to parameterize the crustal velocity model with 7 uniform layers with unknowns velocity (V_p) and thickness values ranging within the boundary extremes reported in Table 2.

We applied the GA using 617 events (associated to 10811 *P*- and 8999 *S*-arrival times) that were selected in order to have an almost homogeneous coverage of the investigated crustal structure. We set the maximum number of iterations equal to 300 and we used populations consisting of 300 individuals. The search is stopped when 70% of generated velocity models had a RMS below a threshold set to 0.12 s. In the upper crust (0-10 km depth) V_p ranges from 5.4 to 6.0 km/s, values that agree with the presence of carbonate rocks that are widely outcropping in central Apennines. In the mid-crust (10-20 km depth) the increase of V_p up to 6.6-6.7 km/s is consistent with the presence of dolomites and evaporites at the bottom of the carbonate platform. The deepest layers are poorly resolved since seismicity concentrates at shallower depths. However, below 20 km depth, the majority of the models show a marked decrease of V_p (5.8 km/s) that may be ascribed to metamorphic formation above the crystalline basement. This result is in good agreement with the 1D V_s model obtained for the inversion of receiver functions for the central Apennines (Chiarabba *et al*., 2010). Another factor behind the anomalous velocity values of the lower crust in the central Apennines might be the existence at lithospheric depths of a slab window below the central-southern Apennines at lithospheric depths (Amato *et al*., 1993; Piromallo and Morelli, 2003; Giacomuzzi *et al*., 2011). This slab window has been explained (Argnani *et al*., 2016) as due to a trench-parallel slab break-off in both the central-southern Apennines and Sicilian Maghrebides, that followed (2 Ma) the soft collision of the outward migrating fold-and-thrust belt into the continental margins of Adria (central-southern Apennines) and Africa (Sicilian Maghrebides).

3.2 Earthquake location

The waveforms of local earthquakes, used to pick arrival times and for hypocenter determination, were extracted from the continuous data stream of the two temporary arrays and merged with those available from the permanent networks. This seismogram collection was performed by using the trigger times, based on standard STA/LTA ratio methods, provided by the RSN and RSA permanent networks, and by station IES1 (Arpino) of the IESN network. In addition, during the two Campoli Appennino swarms (October 2009 and May 2011) and the Sora sequence (February-March 2013), the continuous record of the RSN station POFI (Posta Fibreno), which was located within the epicentral area (Figure 2), was visually scanned. We manually picked the *P*- and *S*-arrival times mostly on the unfiltered seismograms and we assigned a weight to each time pick on the basis of the onsets quality (Table 3).

We detected 7011 earthquakes from January 2009 to December 2013; 741 of these earthquakes were rejected due to their low location quality (Table 4). Figure 4a shows the number of events for each recording station. Compared to the number of events located by only the RSN during the same period (4392 events), we detected 2619 more events, about 37% more. The majority of the 6270 hypocenters (Figure 5a) that we selected with the Hypoellipse location code and using the 1D velocity model obtained with the GA, were located beneath the axis of the Apenninic belt, while relatively less seismic activity was observed along the south-western part of the studied area, along the peri-Tyrrhenian margin, beneath the Frentani Mts., and along the Adriatic coast area (north-eastern edge of the study area). The average RMS residuals of the 6270 selected events is 0.07 s. The final dataset consists of 60638 *P*- and 54565 *S*-wave arrivals (Table 4).

Local magnitude (M_L) was extracted from the INGV earthquake database ISIDe (http://iside.rm.ingv.it/iside/standard/; Working Group, 2010). For the selected events values range from 0.4 to 4.7, and only 33 events show magnitude equal or larger than 3.0. Typically, all

earthquakes exceeding M_L 1.0 were recorded by 8-10 stations, leading to a relatively small azimuthal gap. Earthquakes with smaller magnitudes were usually located with 4-5 stations.
The most challenging part in the localization of seismicity is the accurate determination of hypocenter depths. Thanks to the high station coverage we were able to determine all earthquake hypocenter depths with acceptable uncertainties. For MSA, the more densely covered part, the average station spacing is around 8 km, while for the rest of the study area it is around 15 km. The average location errors for the events located within MSA are 0.7 km (horizontally) and 0.9 km (vertically) with a confidence level of 90%. We detected several small and shallow local earthquakes with a detection threshold of M_L 0.4. Locations errors are significantly larger for seismicity just outside or along the border of the network.
For our selected dataset hypocenter depth extends down to 31 km (four events between 28-31 km depth) with a pronounced maximum between 8 and 12 km (Figure 4b), except a deep M_L 3.2 earthquake at 427 km depth detected in the southern part of the study area. We have computed the fault plane solution of this event, which shows a T-axis indicating a down-dip tension (see Supplementary material). This deep earthquake, together with the December 27, 1978 event of the Gaeta Gulf (M_w 5.9, 387 km depth; Global CMT catalog, Dziewonski *et al*., 1981), is the seismological evidence of the existence and activity of the northern portion of the Tyrrhenian slab beneath the southern Lazio region.

3.3 Seismic swarms and sequences

During the observation period there is clear evidence of swarm activity and of five low-to-moderate magnitude sequences. Figure 5a shows the epicentres of earthquakes belonging to different sequences and swarms depicted with different colours. About 54% of the seismicity is concentrated in the MSA, while the rest is mainly located in the Pontina Plain, southwestern Molise, Fucino area and Sulmona basin. In the following we describe the main characteristics of the seismicity pattern for four sub-areas of the study region. For simplicity's sake we identified these areas with boxes in Figure 5b.

Marsica-Sora area (MSA) (box 1)

Seismicity in MSA is mainly composed by two swarms (SW1 and SW2 in Figures 6a and b) located in the area of Campoli Appennino (October 2009 and May 2011, respectively) and by the largest magnitude sequence detected during our monitoring, with main shock M_L 4.7 (Mw 4.8, Figure 7), on February 16, 2013, to the west of the city of Sora (SE1 in Figures 6a and b). The left cross-section in Figure 6a shows the main shock (white star) for sequence SE1. Figure 8 shows the magnitude-time distribution of SW1, SW2 and SE1. The diagrams for SW1 and SW2 (Figure 8a and b) show that there aren't any clear main shocks, but a series of events with varying magnitudes and rates of activity distributed in time. The figure also clearly shows the tendency of the largest events to strike later, as expected for seismic swarms. The diagram for sequence SE1 shows foreshocks, the M_L 4.7 main shock, followed by an unusual small number of aftershocks. The largest aftershock with M_L 3.2 was followed by only two M_L 2.8. As a matter of fact, in this sequence, only 10 events show magnitude between 2.0 and 3.2.
The SW1 cumulative temporal evolution is characterized by the presence of a steady seismicity rate (~10 day^{-1}) that started after the most active period (October 6-8, 2009) of the burst, lasting approximately 2 weeks. This observation may be consistent with an aseismic slip episode that at least partly released the accumulated tectonic strain (Vidale and Shearer, 2006).
SW1 started on September 30, 2009, with a M_L 3.2 event and lasted one month, with 1309 earthquakes. The maximum local magnitude was M_L 3.6. Within this swarm only 7 events show magnitude equal or larger than 3.0. The swarm was preceded by single M_L 4.2 (M_w 4.0, Val

Comino, Figure 6a) shock on August 6, 2009, located approximately 10 km to the south of the swarm at 13.5 km depth (dark green star in the left cross-section of Figure 6a). The seismicity distribution of the first 8 days of the SW1 delineated a very clear seismic structure dipping to the SW (Figure 6a, right cross-section). During the same period a small swarm, SW3, occurred NNE of SW1.

SW2 (Figure 6a) occurred during May 2011 with 739 events and a maximum local magnitude M_L 2.8. This second swarm was located north-east of the first one. SW1 and SW2 showed a south-west dipping plane (~ 60°, cross section in Figure 6a) with hypocentral depths ranging from 7 to 15 km. These two swarms are slightly shifted from each other by a horizontal gap of ~2 km.

SE1 Sora-Pescosolido sequence started with a M_L 4.7 main shock on February 16, 2013 (Figure 8c), and lasted until the end of March. It was followed by ~ 390 aftershocks. This sequence is formed by three groups of events (left cross-section in Figure 6a). The first and deeper group (~120 events), with hypocentral depths ranging from 14 to 18.6 km, includes the main shock at 18.6 km depth. On the day preceding the main shock, a cloud of small magnitude foreshocks (M_L ranging from 0.9 to 1.6) occurred close to the main shock location at the same hypocentral depth.

The second group (~130 events), shifted to the NE with respect to the first, displays hypocentre depths between 9.5 to 15 km. These two clusters, separated by a gap ~ 2.5 km wide, show a plane dipping to the south-west at ~ 70°. The third group consists of ~140 small shallow earthquakes (depth range 2-8 km), located about 3 km to the north of the main shock epicentre beneath the Ernici Mountains. A small swarm, SW4, occurred few days before SE1 in the Pescasseroli area to the NE.

In addition, two diffuse swarms occurred within MSA (SW5 and SW6, Figure 6b). SW5, a group of 156 events with magnitude M_L ranging from 1.0 to 2.7, occurred beneath the Serra Lunga in Val Roveto, from April 2009 to December 2010, roughly along an E-W direction. The hypocentral depths, in the range 7-11 km, delineates a seismic plane dipping ~ 60° to the NW (cross-section AB in Figure 6b). This cluster is located around 12 km to the NW of the SW1 and SW2 and, as we comment in the next paragraph, it is associated to spatial heterogeneities of the local stress field.

SW6 is a very diffuse swarm of 47 events with maximum magnitude M_L 2.6. Hypocentral depths reach down to 17 km.

Val Comino and south-western Molise (box 2)

On November 26, 2009, in the Val Comino area, approximately 13 km south-east from Campoli Appennino, a small swarm with 15 earthquakes (SW7, Figure 9) M_L ranging 0.8-2.4 and hypocentral depths between 18 and 20 km, occurred. Approximately in the same area, during June-August 2013, other three small swarms (SW8, SW9 and SW10, Figure 9) were detected. These swarms are lined up in a SW-NE direction and are near the location of the 1984 Val Comino seismic sequence (stars in Figure 9). They show hypocentral depth range between 8 and 16 km (AB cross-section in Figure 9), and magnitude M_L from 1.0 to 2.5.

At the end of May 2010, a small sequence of 149 events occurred in two days (29-30 May) within an approximately 5 km^2 area nearby Montaquila village (SE2, Figure 9). The sequence started with an earthquake of M_L 3.3 at 7 km depth. The majority of the aftershocks are concentrated in the 6.4-9.5 km depth range. M_L ranges from 0.5 to 2.4. Cross-section CD in Figure 9 delineates near vertical dipping planes consistent with the pattern of focal mechanisms.

Sulmona Basin, Fucino and Velino-Sirente Mts. (box 3)

Also in this area seismicty is diffused. Worthy of notice is the small sequence SE3 (~20 earthquake, Figure 10), with hypocentral depth around 5 km, that started in March 2009 with two shocks, M_L 3.6 and M_L 3.7, just before the April 6, 2009 L'Aquila main shock, and ended in April with a M_L

3.1 event. Close to Ortona dei Marsi a small cluster (SW11) occurred between March-April 2011. This seismicity, concentrated at 12-14 km depth, is elongated in a NW-SW direction (Figure 10).

Pontina Plain (box 4)

Two seismic sequences occurred in the Pontina Plain on July 2011 and February 2012 (SE4 and SE5, Figure 11). Seismic monitoring of this area is still inadequate due to a lack of RSN stations, low quality deployment sites due to the sedimentary plain, and to the presence of the Tyrrhenian Sea to the west and south-west. SLAM data were available only for the second Pontina Plain sequence. The two main shocks (July 23, 2011, M_L 3.6, 10 km hypocentral depth, and February 15, 2012, M_L 3.5, 18 km hypocentral depth) were felt by the population, probably due to the amplification of ground motion by the plain sediments, and produced some degree of anxiety. With the exclusion of the two main shocks, the local magnitudes of the 40 located events range from 1.0 to 2.8, while hypocentral depth is between 4 and 18 km.

3.4 Focal mechanisms and stress inversion analysis

Fault plane solutions were derived for a total of 759 earthquakes. For this analysis we used the same combined waveform data set (RSN + RSA + local temporary array) developed for the event location. *P*-wave polarities were determined manually and picked on the raw seismograms. The orientation of the nodal planes was determined by using the FPFIT code (Reasenberg and Oppenheimer, 1985). From the focal mechanisms dataset we selected the most constrained solutions on the basis of the values of Q_f and Q_p, the two FPFIT output quality factors (Table 5). Q_f gives information about the solution misfit of the polarity data F_j, whereas Q_p reflects the solution uniqueness in terms of the 90% confidence region for strike (Δs), dip (Δd) and rake (Δr). The quality factors range from A to C for decreasing quality. All focal mechanism with one or both quality factors C, and with less than 12 polarities, were rejected. Out of the 759 focal mechanism computed, we selected 468 solutions well constrained by 12 or more observations homogenously distributed on the focal sphere (Figure 5b; see Supplementary material). The majority of the selected focal mechanisms (Figure 12) represent pure normal faults (63.7%) and normal faults with strike-slip component (18.2%), whereas the 12.2% are pure strike-slip mechanisms. Only a 1.7% are given by reverse with strike-slip component and 0.4% pure reverse fault-plane solutions. The remaining 3.8% are odd mechanisms. The orientations of the T-axis of normal and strike-slip solutions suggests a widespread NE-SW extension regime. The only two pure inverse solutions (~16 km depth, M_L 2.5 and 2.1) are located at the north-west edge of the Maiella Massif (Figure 10).

Crustal stress orientations provide important information on the mechanics of regional deformation. Numerous methods exist for inverting earthquake focal mechanisms for stress orientation, and the more widely used methods usually obtain similar results for similar data sets (Angelier, 1979, 1984; Gephart and Forsyth, 1984; Michael, 1984, 1985, 1987; Rivera and Cisternas, 1990). We performed stress field inversions applying the FMSI (Focal Mechanism Stress Inversion) code developed by Gephart and Forsyth (1984) (Gephart,1990a; Gephart,1990b) which provides accurate estimates of the stress tensors. This method resolves four of the six independent components of the stress tensor, commonly parameterized by three unit vectors, the maximum, minimum and intermediate compressive principal stress axis orientations (σ_1, σ_3 and σ_2), and the dimensionless parameter $R = (\sigma_2 - \sigma_1)/(\sigma_3 - \sigma_1)$ which describes the relative magnitudes of the principal stresses and hence constrains the shape of the stress ellipsoid. Discrepancies between the stress tensor orientation and the observed data are defined by a misfit measure. The misfit is given by the angular difference between the observed slip direction on a fault plane and the shear stress on the same fault plane that is derived from a given stress tensor.

We applied the stress field inversion method to the good quality dataset of the MSA. The focal mechanism ensemble was subdivided into three subsets according to the three main seismic swarm/sequences. The first inversion (Figure 13a) was carried out with the 65 fault plane solutions calculated for the SW1 (October 2009). The average misfit is 5.1° with a horizontal (plunge 0°) (Table 6) NNE-SSW oriented minimum stress axis (σ_3) and a vertical σ_1 (plunge 86°). Stress ratio R is 0.5. The second inversion (Figure 13b) is based on 34 focal mechanisms of the SW2 (May 2011). The average misfit is 3.6°, and the maximum stress axis (σ_1) is sub-vertical (plunge 71°). The stress ratio R near the solution is 0.7, implying that σ_2 is slightly close in its absolute value to σ_3. For this inversion we find a clockwise rotation of the σ_3 which is sub-horizontal (plunge 5°) but E-W oriented. The third inversion (Figure 13c) was performed using the 39 fault plane solutions of the SE1 (February-March 2013). Average misfit is 4.5° and the stress ratio R is 0.5, as in the first inversion. This sequence is slightly shifted to the W and NW with respect to the SW1 and SW2. In this inversion the minimum stress axis (σ_3) is horizontal (plunge 1°) and NE-SW oriented, while the σ_1 is near the vertical (plunge 74°).
These results clearly show that the MSA is affected by an extensional stress regime along NE-SW. The low values of average misfit in the three inversion procedures suggest a homogeneous stress distribution within the area. We also applied the Gephart method using the 23 fault plane solutions of the Serra Lunga cluster (SW5, Figure 13d), which is located around 12 km N-W of the SW1 and SW2. In this small dataset strike-slip solutions are predominant. In general, the inversion results are consistent with a NE-SW Apenninic extension stress regime (σ_3 sub-horizontal NE-SW directed), but the ENE-WSW striking nodal planes suggest a transcurrent right-lateral stress regime (σ_1 horizontal with a NW-SE direction) in the small Serra Lunga area.

4. Discussion

The central Apennines present one of the highest seismic hazard levels in Italy (Akinci *et al*., 2009). In fact, many destructive events in this area are filed in the historical catalogue (CPTI15, Rovida *et al*., 2016). At present, crustal faulting and seismicity result from the ongoing extensional tectonics.
Seismicity in the sector of the central Apennines we are investigating often takes place as diffuse swarm activity and low-to-moderate magnitude seismic sequences. Swarms have often been found to be shallow sequences (usually characterized by frequent small/moderate events and by hypocentre migration in time and space) along normal faults. Earthquake swarms and seismic sequences occur every year in Italy, particularly along the Apennines. Recent examples are the 2009 L'Aquila seismic sequence, preceded by an extended series of small earthquakes recorded before the M_w 6.1 main shock (Chiarabba *et al*., 2009; Valoroso *et al*., 2013), the April 2010 Pietralunga sequence (Gubbio basin, northern Apennines; Marzorati *et al*., 2014), and the 2010-2014 swarm-like seismic sequence in the Pollino Range (southern Apennines, Passarelli *et al*., 2015). Given the absence of recent large earthquakes in the region, the pattern of seismicity we observe might be consistent with a fragmented tectonic scenario in which faults with small dimensions release seismic energy in a diffused way.

Seismicity and stress regime

The spatial and temporal behaviour of the seismicity in the MSA area is consistent with the general characteristics of swarm-like seismicity (Vidale and Shearer, 2006; Hainzl *et al*., 2012). The swarm activity in the MSA is similar to the one observed in the Pollino Range (southern Apennines; Passarelli *et al*., 2015), given its long-lasting seismic release and moderate magnitude of the largest shocks (M_L 4.7 in our case, 5.1 in the Pollino sequence). Swarm/sequences occurred in proximity of the major mapped faults, the Upper Sangro Valley fault in the MSA (estimated length 20 km, minimum vertical slip rate 0.17-0.21 mm/yr, horizontal slip rate 0.14-0.18 mm/yr; Galadini and

Galli, 2000), the Alto Tiberina fault in the Gubbio basin (northern Apennines; Marzorati *et al*., 2014) and the Pollino fault in the Pollino Range (southern Apennines; Passarelli *et al*., 2015). In all these cases, the relocation of seismicity depicts a complex geometry of the activated faults. Swarm activity is usually explained by fluid infiltration at crustal depth (5-20 km depth) or pore pressure diffusion within the seismogenic zone (Hainzl *et al*., 2012), reducing normal stress levels along existent faults. The recent study by Fischer *et al*., (2010) on the 2008 West Bohemia earthquake swarms, shows similarities with the MSA swarms, such as their maximum magnitude (3.8), depth extension (6-13 km). Furthermore, the steeply dipping fault planes delineated by the hypocentre distributions are also a common feature of the Nový Kostel (West Bohemia/Vogtland) and MSA (central Italy) “swarm regions”.

The Plio-Quaternary tectonic extension process within the inner zone of the Apenninic belt, is associated with diffuse carbon dioxide degassing (Chiodini *et al*., 2004). Whether the CO_2 has a metamorphic and/or magmatic upper crust origin is debated (Minissale *et al*., 2000; Chiodini *et al*., 2004; Minissale, 2004; Heinicke *et al*., 2006). High fluid pressures encountered at shallow crustal depth suggest that deep fluids from deeper layers could play a key role in triggering earthquakes (Chiodini *et al*., 2004; Antonioli *et al*., 2005) and might also control the spatio-temporal evolution of the seismicity (Piccinini and Antonioli, 2007).

The seismicity pattern in the MSA (Figure 6a, box 1) is associated to the western normal fault system of the central Apennines (this study and Galadini and Galli, 2000). A recent study on the background seismicity found at the border between central and southern Apennines (Milano *et al.*, 2008) shows that it is generated as low magnitude earthquakes (less than 3.0) by NE-SW striking faults that move in response to a second-order NW-SE extension. Moreover, aftershock fault plane solutions computed by Milano and Di Giovambattista (2011) in a re-evaluation of the Val Comino 1984 earthquake, show normal dip-slip solutions with planes striking NE-SW. We find another evidence of the existence of a second-order extension given by the four pure normal solutions for earthquakes localized between central and southern Apennines, in which the T-axis is E-W striking. The maximum magnitude of these events is 2.7 and hypocentral depth is ranging between 7.4 and 9.1 km (green-gray fault plane solutions in the center-right of Figure 9).

We note the striking similarity between the patterns of focal mechanisms in the MSA and in West Bohemia/Vogtland (Fischer *et al*., 2010), which indicate extensional regimes with T-axis in the NE-SW direction. For both areas, this appears consistent with the axis’s orientation of regional tectonic stresses, suggesting that faulting during individual swarms is controlled mainly by the regional stress field.

Several fault plane solutions in our study show right-lateral strike-slip motion. The most important cluster displaying this kinematics is the one located beneath the Serra Lunga in the Marsica area (SW5, Figure 6b). Events are concentrated within 9-11 km depth range. T-axes are sub-horizontal and NNE-SSW striking, while the probable fault plane of these solutions is identified with the ENE-WSW striking plane. In fact, the seismicity, which occurred in the period 2009-2010, delineates an approximately E-W striking structure. This group of small strike-slip faults could be interpreted as a secondary transfer zone in a region that is dominated by NE-SW extension. Their location probably corresponds to the tips of the main NW-SE striking normal faults that are responsible for the historical large earthquakes in the central Apennines. Right-lateral strike-slip motion is also inferred by other focal mechanisms of events located in the Abruzzo Apennines (dark green fault plane solutions, SE3 in Figure 10), as also observed by Bagh *et al*. (2007).

There is a change from the right-lateral strike-slip kinematics in the Gargano-Apulia foreland (Del Gaudio *et al*., 2007) and Frentani Mountains (2002 Molise earthquake; Di Luccio *et al*., 2005) to the NW-SE striking normal faults of the inner Apenninic belt. This passage is marked by the four right-lateral strike-slip focal mechanisms which delineate the western limit of the strike-slip regime (dark green and brown solutions, upper-right corner of Figure 9). All solutions show a ENE-WSW nodal plane consistent with a right-lateral motion, and a NE-SW striking T-axis. These events have a depth ranging from 16 to 21 km with a maximum magnitude M_L 3.2. The pattern of the active deformation in the eastern Molise region (2002 earthquake) and in this portion of the study area (Western Molise), where we find E-W right-lateral strike-slip motion, is explained in terms of the relative motion between the two Adria microplates, the northern rotating around an Eulerian pole located at the western margin of the Po valley, and the southern, which includes the Apulian promontory and the Ionian Sea, rotating in the opposite direction (D'Agostino *et al*., 2008).

The only two pure thrust solutions computed in this work (pale blue solutions in the upper-right corner in Figure 10) belong to events localized in the north-eastern edge of the study area (Sulmona basin, box 3), not far away from the active extension zone of the Apenninic belt. The two events (M_L 2.5 and 2.1) show an hypocentral depth of 16 km. We interpret this as an evidence of the active NE-compression along the Adriatic coast sector (Montone and Mariucci 2016, and reference therein). This example shows that, in agreement with worldwide observations (Yang and Hauksson, 2013), the zone that marks the passage from one state of stress to another may extend only a few kilometres.

The western and south-western margin of the Apenninic belt and the peri-Tyrrhenian sector (box 4) are affected by scarce seismicity, generally located at shallow depths. During our survey we only detected two small seismic sequences in the Pontina Plain (pale blue and green dots in Figure 11). Hypocentral depth, which is ranging from 6 to 18 km, is poorly constrained due to the lack of seismic stations in this region. The magnitude of the two main shocks is 3.6 (July 23, 2011) and 3.5 (February 15, 2012). Fault plane solutions show a left-lateral strike-slip motion along the NNE-SSW striking nodal plane. We interpret this seismicity as belonging to a N-S shear zone in the Pontina Plain, which is bordered to the east by the Apenninic NE-SW extension zone. This kinematics is also found in the greater Rome area (Frepoli *et al*., 2010) NW of the study area (Figure 5b). The widespread NE-SW extension regime is confirmed by the normal focal mechanism of the main Alban Hills earthquake (M_L 3.5), together with the fault plane solutions of the smaller earthquakes.

Seismic potential in the MSA

This area was struck in 1654 by an M_w ~ 6.2 destructive event. At present, there are no conclusive data available for the identification of the responsible seismogenic source (Carrara *et al*., 1995). It is possible that the 1654 earthquake was produced by a blind fault. Establishing the seismogenic layer thickness and the amount of the potential seismic energy that can be released, can help identify the most likely locations where such destructive earthquakes might nucleate.

The hypocentral depth of the most important event that occurred within our observing period, the M_L 4.7, 18.6 km depth Sora earthquake, is consistent with the 18 km depth of the Brittle-Ductile Transition (BDT) in the crust beneath the central Apennines, estimated by Petricca *et al*. (2015, and reference therein). Their estimation is based on a simplified two-layer crustal composition with quartz rheology for the upper crust and a diabase rheology for the lower crust, and on the heat flow map produced by Della Vedova *et al*. (2001) and Petricca *et al*. (2013). Earthquakes magnitude associated to normal faults increases with BDT depth.

The graviquake model (Doglioni *et al*., 2013) can help us estimate the expected maximum earthquake magnitude in an extensional setting. The main energy source for hangingwall fault collapsing (i.e., normal fault earthquakes) is gravity. The maximum amount of gravitational potential energy that can be released as an earthquake, increases with the volume of the collapsing crustal rock, the dip of the fault and the static friction of involved rocks. Steeper normal faults are able to release more energy due to a larger vertical displacement (Doglioni *et al*., 2011; 2013).

Petricca *et al*. (2015) compared the magnitude of the Italian extensional earthquakes with the dip of the faults and they found that steeper faults are characterized by earthquakes with lower frequency of occurrence and larger magnitude. From the aftershock distribution and from the fault plane dip (~ 65°) of the February 16, 2013 main shock, we infer that in the Marsica area normal faults are characterized by steep fault plane. On the basis of the computations by Petricca *et al*. (2015, Figure 11) given our estimated depth of the BDT of 18 km and a normal fault dip > 60°, we can estimate a maximum expected magnitude M ~ 7 earthquake for the MSA.

Our analysis confirms the widespread NE-SW extensional regime that characterize the slowly deforming region of the northern-central Apennines. The accommodation of the present-day extension is performed, however, through both normal (the majority, over 80%) and transcurrent (over 10%) strike-slip faults. D'Agostino (2014), by comparing estimates of tectonic strain rates derived from dense Global Positioning System measurements with the recurrence of seismicity in the last ~ 500 years, observes a reduced seismic release between the epicentrals areas of the 1805 and 1915 earthquakes (central Apennines). The expected release of cumulated deformation needed to match the reduced past seismic release, may cause a M_w ~ 6.9 earthquake in the central Apennines (D'Agostino, 2014), a value that is in agreement with the previous estimate obtained by using the graviquake model.

At present it is difficult to say if the swarms are accompanied by a large aseismic release of geodetic moment and if the low-seismicity fault portions are linked to creeping and/or to locked faults. To improve our knowledge on the way seismic energy is released in the central Apennines accurate location of seismicity should be complemented by other observations, such as the correlation between the *b*-values and the seismic rate, measurements on changes of velocity of seismic wave in the crust, high resolution geodetic monitoring, and knowledge of the physico-chemical properties of fluids in wells and thermal- and hot-springs.

5. Conclusions

We examined the seismicity of a wide portion of central Italy by analyzing more than 60.000 waveforms recorded during two temporary passive experiments in a five-year period. The bulk of activity is represented by several low-magnitude seismic sequences and swarms spatially concentrated within an area of about 50 km^2. Most of the relocated hypocenter distributions highlight clear seismogenic structures that extend in the upper-middle crust of the central Apennines and neighbouring regions down to ~20 km.

In this area, where an extensional stress field dominates, the observed stress patterns are compatible with both transcurrent and extensional tectonic regimes. The majority of the selected fault plane solutions represent pure normal faults and normal faults with strike-slip component (81.9%), while the pure strike-slip solutions are 12.2%.

The source geometries that we derived show that there are abrupt changes in the stress pattern within only a few kilometres, suggesting a structural complexity in this area. The seismicity and stress distribution we observe might be consistent with a fragmented tectonic scenario in which faults with small dimensions release seismic energy in a diffused way, in the absence of large earthquake.

The low-to-moderate diffuse seismicity we studied could represent the partial, incomplete response to the estimated stress accumulated due to the present tectonic setting. In particular, we found that the MSA is a potential candidate location for large earthquakes. Hypocentral locations are consistent with the depth of the Brittle-Ductile Transition (BDT), about 18 km within this section of the central Apennines crust. Moreover, in the MSA, normal faults are characterized by steep fault planes, which might increase the seismic potential as predicted by the graviquake model.

Future investigations are planned to extend this analysis by including, for instance, the more recent seismicity, and by performing complementary information (e.g., *b*-value study and seismic tomography).

Aknowledgments

The SLAM project was supported by the Centro Nazionale Terremoti (INGV). We thank the personnel of the INGV Seismic Mobile Network for providing instrumentation and Aladino Govoni for archiving the data. A great thank to E. Giandomenico for his help in the management of the SLAM stations and M. Pascolini for technical assistance with the regional seismic network of Abruzzo (RSA). We are grateful to the Centro Funzionale Regionale – Agenzia Regionale di Protezione Civile of the Molise region for providing us the parametric data of the Molise regional seismic network and to the persons involved with the Italian Earthquake Seismic Network (IESN), for providing their digital seismograms. We thank also G. Milana for the Arpino digital station waveforms. Furthermore, we would like to thank all people which helped us find sites for the temporary stations in the provinces of Frosinone, Latina, L'Aquila and Isernia, and for the regional network of Abruzzo (RSA). We thank L. Margheriti and C. Doglioni for their encouragement. The figures were produced with the GMT software (Wessel *et al*., 2013). One of the authors (AF) dedicates this work to the memory of Francesco (Checco) Bedognè.

Appendix A. Supplementary material

The whole focal mechanism data set is provided as supplementary material.

References

Akinci, A., Galadini, F., Pantosti, D., Petersen, M.D., Malagnini, L., Perkins, D., 2009. Effect of time dependance on probabilistic seismic-hazard maps and deaggregation for the central Apennines, Italy. Bull. Seismol. Soc. Am., 99, 585-610, doi:10.1785/0120080053.

Amato, A., Alessandrini, B., Cimini, G.B., Frepoli, A., Selvaggi, G., 1993. Active and remnant subducted slabs beneath Italy: evidence from seismic tomography and seismicity. Annals of Geophysics, 36 (2), 201-214.

Amoruso, A., Crescentini, L., Scarpa, R., 1998. Inversion of source parameters from near and far field observations: An application to the 1915 Fucino earthquake, central Apennines. J. Geophys., Res., 103, 29,989-29,999, doi:10.1029/98JB02849.

Anderson, H., Jackson, J., 1987. Active tectonics of the Adriatic region. Geophysical Journal International, 91 (3), 937-983.

Angelier, J., 1979. Determination of the mean principal directions of stresses for a given fault population, Tectonophysics, 56, 17-26.

Angelier, J., 1984. Tectonic analysis of fault slip data sets, J. Geophys. Res., 89, 5835-5848.

Antonioli A., Piccinini D., Chiaraluce L., Cocco M., 2005. Fluid flow and seismicity pattern; evidence from the 1997 Umbria-Marche (central Italy) seismic sequence. Geophys. Res. Lett., 32/10, 4 pp.

Argnani, A., Cimini G.B., Frugoni F., Monna S., Montuori C., 2016. The role of continental margins in the final stages of arc formation: Constraints from teleseismic tomography of the Gibraltar and Calabrian Arc (Western Mediterranean), Tectonophysics, 677-678, 135-152, doi:10.1016/j.tecto.2016.03.037.

Basili, R., Valensise G., Vannoli P., Burrato P., Fracassi U., Mariano S., Tiberti M.M., Boschi E., 2008. The database of individual seismogenic sources (DISS), version 3: summarizing 20 years of research on Italy's earthquake geology, Tectonophysics, 453, no. 1-4, 20-4.

Bagh, S., Chiaraluce, L., De Gori, P., Moretti, M., Govoni, A., Chiarabba, C., Di Bartolomeo P., Romanelli, M., 2007. Background seismicity in the central Apennines of Italy: The Abruzzo region case study. Tectonophysics, 444, 80-92, doi:10.1016/j.tecto.2007.08.009.

Boncio, P., Lavecchia, G., Pace, B., 2004. Defining a model of 3D seismogenic sources for Seismic Hazard Assessment applications: The case of central Apennines (Italy). J. Seismol., 8, 407-425, doi:10.1023/B:JOSE.0000038449.78801.05.

Carrara, C., Dal Pra G., Giraudi C., 1995. Lineamenti di tettonica plioquaternaria dell'area, in *Lazio Meridionale, Sintesi delle Ricerche Geologiche Multidisciplinari*, Dipartimento Ambiente, ENEA, Rome, 151-155.

Cavinato, G.P., Carusi, C., Dall'Asta, M., Miccadei, E., Piacentini, T., 2002. Sedimentary and tectonic evolution of Plio-Pleistocene alluvial and lacustrine deposits of Fucino Basin (central Italy). Sedimentary Geology, 148, 29-59.

Chatelain, J.L., 1978. Etude fine de la sismicité en zone de collision continentale à l'aide d'un réseau de stations portables: la region Hindu-Kush-Pamir. Thèse de 3 éme cycle, Univ. Paul Sabatier, Toulouse.

Chiarabba, C., et al., 2009. The 2009 L'Aquila (central Italy) Mw 6.3 earthquake: Main shock and aftershocks. Geophys. Res. Lett., 36, L18308, doi:10.1029/2009GL039627.

Chiarabba, C., Bagh, S., Bianchi, I., De Gori, P., Barchi, M., 2010. Deep structural heterogeneities and the tectonic evolution of the Abruzzi region (Central Apennines, Italy) revealed by microseismicity, seismic tomography, and teleseismic receiver functions. Earth Planet. Sci. Lett., 295, 462-476, doi:10.1016/j.epsl.2010.04.028.

Chiodini G., Cardellini C., Amato A., Boschi E., Caliro S., Frondini F., Ventura G., 2004. Carbon dioxide earth degassing and seismogenesis in central and southern Italy. Geophys. Res. Lett., 31, L07615, doi:10.1029/2004GL019480.

Cimini, G.B., De Gori, P., Frepoli, A., 2006. Passive seismolgy in southern Italy: the SAPTEX array, Ann. Geophys., 49 (2/3), 825-840.

Cimini, G.B., Frepoli, A., De Luca, G., Pagliuca, N.M., Marchetti, A., Giandomenico, E., 2013. Studio della sismicità nell'area tra Lazio, Abruzzo e Molise – l'esperimento di sismica passiva del progetto SLAM, Rapporto Tecnico n. 255, Istituto Nazionale di Geofisica e Vulcanologia, Roma.

D'Addezio, G., Masana G., Pantosti D., 2001. The Holocene paleoseismicity of the Aremogna-Cinque Miglia fault (central Italy), J. Seism., 5, 181-205.

D'Agostino, N., 2014. Complete seismic release of tectonic strain and earthquake recurrence in the Apennines (Italy), Geophys. Res. Lett., 41, doi:10.1002/2014GL059230.

D'Agostino, N., Avallone, A., Cheloni, D., D'Anastasio, E., Mantenuto, S., Selvaggi, G., 2008. Active tectonics of the Adriatic region from GPS and earthquake slip vectors. J. Geophys. Res., 113, B12413, doi:10.1029/2008JB005860.

D'Agostino, N., England, P., Hunstad, I., Selvaggi, G., 2014. Gravitational potential energy and active deformation in the Apennines. Earth Planet. Sci. Lett., 397, 121-132, doi:10.1016/j.epsl.2014.04.0130012

Del Gaudio, V., Pierri, P., Frepoli, A., Calcagnile, G., Venisti, N., Cimini, G.B., 2007. A critical revision of the seismicity of northern Apulia (Adriatic microplate - southern Italy) and implications for the identification of seismogenic structures, Tectonophysics 436, 9-35, doi:10.1016/j.tecto.2007.02.013.

Della Vedova, B., Bellani, S., Pellis, G., Squarci, P., 2001. Deep temperatures and surface heat flow density distribution. In: Vai, G.B., Martini, P. (Eds.), Anatomy of an Orogen: The Apennines and Adjacent Mediterranean Basins. Kluwer Academic Publishers, Dordrecht, Netherlands, pp. 65-76.

Del Pezzo, E., De Natale, G., Iannacone, G., Martini, M., Scarpa, M., Zollo, A., 1985. Analisi preliminare della sequenza sismica dell'Abruzzo mediante dati di una rete sismica digitale. Proc. 4° Meeting GNGTS, Rome 1985, pp. 79-96.

De Luca, G., Cattaneo, M., Monachesi, G., Amato, A., 2009. Seismicity in central and northern Apennines integrating the Italian national and regional networks, Tectonophysics, doi:10.1016/j.tecto.2008.11.

De Mets, C., Gordon, R.G., Argus, D.F., Stein, S., 1994. Current plate motions. Geophys. J. Int., 101, 425-478.

Di Luccio, F., Fukuyama, E., Pino, N.A., 2005. The 2002 Molise earthquake sequence: What can we learn about the tectonics of southern Italy? Tectonophysics, 405, 141-154, doi:10.1016/j.tecto.2005.05.024.

Doglioni, C., 1993. Some remarks on the origin of foredeeps. Tectonophysiscs, 228, 1-20.

Doglioni, C., Barba, S., Carminati, E., Riguzzi, F., 2011. Role of the brittle-ductile transition on fault activation. Phys. Earth Planet. Int., 184, 160-171, http://dx.doi.org/10.1016/j.pepi.2010.11.005.

Doglioni, C., Carminati, E., Petricca, P., Riguzzi, F., 2013. Normal fault earthquakes or graviquakes. Sci. Rep. 5:12110, 1-12. http://dx.doi.org/10.1038/srep12110.

Dziewonski, A.M., Chou, T.A., Woodhouse, J.H., 1981. Determination of earthquake source parameters from waveform data for studies of global and regional seismicity. J. Geophys. Res., 86, 2825-2852. doi:10.1029/JB086iB04p02825.

Fischer, T., Horálek, J., Michálek, J., Boušková, A., 2010. The 2008 West Bohemia earthquake swarm in the light of the WEBNET network, J. of Seis., 14.665-682, doi:10.1007/s10950-010-9189-4.

Frepoli, A., Marra, F., Maggi, C., Marchetti, A., Nardi, A., Pagliuca, N.M., 2010. Seismicity, seismogenic structures, and crustal stress fields in the greater Rome area (central Italy). J. Geophys. Res., 115, B12303, doi:10.1029/2009JB006322.

Galadini, F., Galli, P., 2000. Active tectonics in the central Apennines (Italy) – Input data for seismic hazard assessment. Nat. Hazards, 22, 225-270, doi:10.1023/A:1008149531980.

Gephart, J. W., 1990a. FMSI: a Fortran program for inverting fault/slickenside and earthquake focal mechanism data to obtain the regional stress tensor, Computers and Geosciences, 16, 953-989, doi:10.1016/0098-3004(90)90105-3.

Gephart, J. W., 1990b. Stress and the direction of slip on fault planes, Tectonics, 9, 845-858.

Gephart, J.W., Forsyth D.W., 1984. An improved method for determining the regional stress tensor using earthquake focal mechanism data: application to the San Fernando earthquake sequence, J. Geophys. Res., 89, 9305-9320.

Giacomuzzi, G., Chiarabba, C., De Gori, P., 2011. Linking the Alps and Apennines subduction system: new constraints revealed by high-resolution teleseismic tomography. Earth Planet. Sci. Lett., 301, 531-543, doi:10.1016/j.epsl.2010.11.033.

Hainzl S., Fischer T., Dahm T., 2012. Seismicity-based estimation of the driving fluid pressure in the case of swarm activity in Western Bohemia. Geophys. J. Int., 191 (1), 271-281.

Heinicke J., Braun T., Burgassi P., Italiano F., Martinelli G., 2006. Gas flow anomalies in seismogenic zones in the upper Tiber Valley, central Italy. Geophys. J. Int., 167/2, 794-806.

Hensch M., Riedel C., Reinhardt J., Dahm T., The NICE-People, 2008. Hypocenter migration of fluid-induced earthquake swarms in the Tjörnes Fracture Zone (North Iceland). Tectonophysics, 447, 80-94.

Holland, J.H., 1975. Adaptation in Natural and artificial systems. University of Michigan Press, Ann Arbor.

ISIDe Working Group, 2010. Italian Seismological Instrumental and parametric Database, http://iside.rm.ingv.it.

Jenny S., Goes S., Giardini D., Kahle H.G., 2006. Seismic potential of Southern Italy. Tectonophysics, 415, 81-101, doi:10.1016/j.tecto.2005.12.003

Jolivet, L., Faccenna, C., Goffe, B., Mattei, M., Rosseti, F., Brunet, C., Storti, F., Funiciello, R., Cadet, J.P., D'Agostino, N., Parra, T., 1998. Midcrustal shear zones in postorogenic extension: example from the northern Tyrrhenian Sea. Journal of Geophysical Research, 103 (B6), 12123-12160.

Lahr, J.C., 1989. HYPOELLIPSE/Version 2.0: a computer program for determining local earthquake hypocentral parameters, magnitude and first-motion pattern, U.S. Geol. Surv. Open-file Report, 95, 89-116.

Marzorati S., Massa M., Cattaneo M., Monachesi G., Frapiccini M., 2014. Very detailed seismic pattern and migration inferred from the April 2010 Pietralunga (northern Italian Apennines) micro-earthquake sequence, Tectonophysics, 610, 91-109.

Michael, A., 1984. Determination of stress from slip data: Faults and folds, J. Geophys. Res., 89, 11517-11526.

Michael, A., 1985. Regional stress and large earthquakes: An observational study using focal mechanisms, Ph.D. thesis, Stanford Univ., California.

Michael, A., 1987. Use of focal mechanisms to determine stress: A control study, J. Geophys. Res., 92, 357-368.

Milano, G., Di Giovambattista, R., 2011. Seismicity at the border between central and southern Apennines (Italy): Re-evaluation of the early 1984 instrumental earthquake. Tectonophysiscs, 499, 92-104.

Milano, G., Di Giovambattista, R., Ventura, G., 2008. Seismic activity in the transition zone between southern and central Apennines (Italy): Evidences of longitudinal extension inside the Ortona-Roccamonfina tectonic line. Tectonophysics, 457, 102-110.

Minissale A., Magro G., Martinelli G., Vaselli O., Tassi G.F., 2000. Fluid geochemical transect in the Northern Apennines (central-northern Italy); fluid genesis and migration and tectonic implications. Tectonophysics, 319/3, 199-222.

Minissale A., 2004. Origin, transport and discharge of CO_2 in central Italy. Earth-Science Reviews, 66/1-2, 89-141.

Montone, P., Mariucci, M.T., Pondrelli, S., Amato, A., 2004. An improved stress map for Italy and surrounding regions (central Mediterranean). J. Geophys. Res., 109 (B10410), doi: 10.1029/2003JB002703.

Montone, P., Mariucci, M.T., 2016. The new release of the Italian contemporary stress map, Geophys. J. Int., 205, 1525-1531, doi: 10.1093/gji/ggw100.

Moretti, M., Chiarabba, C., Cianchini, G., Colasanti, G., Criscuoli, F., De Gori, P., Frepoli, A., Govoni, A., Marchetti, A., Serratore, A., 2011. Emergenza sismica nel Frusinate (Ottobre 2009 – Gennaio 2010): l'intervento della Rete Sismica Mobile *stand-alone* e l'analisi dati, Rapporto Tecnico n. 200, Istituto Nazionale di Geofisica e Vulcanologia, Roma.

Pace, B., Boncio, P., Lavecchia G., 2002. The 1984 Abruzzo earthquake (Italy): an example of seismogenic process controlled by interaction between differently oriented synkinematic faults, Tectonophysics, 350, 237-254.

Palano, M., 2015. On the present-day crustal stress, strain-rate fields and mantle anisotropy pattern of Italy. Geophys. J. Int., 200 (2), 969-985, doi:10.1093/gji/ggu451.

Pantosti, D., D'Addezio, G., Cinti, F., 1996. Paleoseismicity of the Ovindoli-Pezza fault, central Apennines, Italy: A history including a large previously unrecorded earthquake in the Middle Age (860-1300 A.D.). J. Geophys. Res., 101, 5937-5959, doi:10.1029/95JB03213.

Papanikolaou, I.D., Roberts, G.P., Michetti, A.M., 2005. Fault scarps and deformation rates in Lazio-Abruzzo, central Italy: Comparison between geological fault slip rate and GPS data. Tectonophysics, 408, 147-176, doi:10.1016/j.tecto2005.05.043.

Passarelli L., Hainzl S., Cesca S., Maccaferri F., Mucciarelli M., Roessler D., Corbi F., Dahm T., Rivalta E., 2015. Aseismic transient driving the swarm-like seismic sequenze in the Pollino range, Southern Italy. Geophys. J. Int., 201, 1553-1567, doi:10.1093/gji/ggv111.

Patacca, E., Scandone, P., 1989. Post-Tortonian mountain building in the Apennines. The role of the passive sinking of a relic lithospheric slab. In: Boriano, A., Bonafede, M., Piccardo, G.B., Vai, G.B. (Eds.), The lithosphere in Italy: Atti Conv. Lincei, 80, pp. 157-176.

Patacca, E., Sartori, R., Scandone, P., 1990. Tyrrhenian Basin and Apenninic Arcs: kinematics relations since late Tortonian times. Memorie della Società Geologica d'Italia, 45, 425-451.

Petricca, P., Carafa, M.M.C., Barba, S., Carminati, E., 2013. Local, regional and platescale sources for the stress field in the Adriatic and Periadriatic region. Mar. Pet. Geol., 42, 160-181, http://dx.doi.org/10.1016/j.marpetgeo.2012.08.005.

Petricca, P., Barba, S., Carminati, E., Doglioni, C., Riguzzi, F., 2015. Graviquakes in Italy, Tectonophysics, 656, 202-214, http://dx.doi.org/10.1016/j.tecto.2015.07.001.

Piccinini D., Antonioli A., 2007. Parametri di sorgente della sequenza Umbro-Marchigiana: diffusione di fluidi o interazioni di sforzo statico. Workshop: Dieci anni dopo il terremoto dell'Umbria-Marche: stato delle conoscenze sulla sismogenesi in Italia. Camerino, 26-27 Giugno 2007.

Piromallo, C., Morelli, A., 2003. *P* wave tomography of the mantle under the Alpine-Mediterranean area. J. Geophys. Res., 108 (B2), 2065. doi:10.1029/2002JB001757.

Reasenberg, P., Oppenheimer, D., 1985. FPFIT, FPPLOT and FPPAGE: FORTRAN computer programs for calculating and displaying earthquake fault plane solutions, USGS Open-file Report, 85-730, 109.

Rivera, L., Cisternas, A., 1990. Stress tensor and fault plane solutions for a population of earthquakes, Bull. Seismol. Soc. Am., 80, 600-614.

Roberts, G.P., Michetti, A.M., 2004. Spatial and temporal variations in growth rates along active normal faults systems: An example from the Lazio-Abruzzo Apennines, central Italy, J. Struct. Geol., 26, 339-376, doi:10.1016/S0191-8141(03)00103-2.

Romano, M.A., De Nardis, R., Garbin, M., Peruzza, L., Priolo, E., Lavecchia, G., Romanelli, M., 2013. Temporary seismic monitoring of the Sulmona area (Abruzzo, Italy): a quality study of microearthquake locations, Nat. Hazards Earth Syst. Sci., 13, 2727-2744, doi:10.5194/nhess-13-2727-2013.

Rovida A., Locati M., Camassi R., Lolli B., Gasperini P. (eds), 2016. CPTI15, the 2015 Version of the Parametric Catalogne of Italian Earthquakes (Milano, Bologna, http://emidius.mi.ingv.it/CPTI. http://dx.doi.org/10.6092/INGV.IT-CPTI15.

Sambridge, M., and K. Gallagher, 1993. Earthquake hypocenter location using genetic algorithms. Bull. Seism. Soc. Am., vol. 83, no. 5, 1467-1491.

Serri, G., Innocenti, F., Manetti, P., 1993. Geochemical and petrological evidence of the subduction of delaminated Adriatic continetal lithosphere in the genesis of the Neogene-Quaternary magmatism of central Italy, Tectonophysics, 223, 117-147, doi:10.1016/0040-1951(93)90161-C.

Trnkoczy, A., Bormann, P., Hanka, W., Holcomb, L.G., Nigbor, L.R., Shinohara, M., Suyehiro, K., Shiobara, H., 2012. Site selection, preparation and installation of seismic stations. In: New Manual of Seismological Observatory Practice (NMSOP-2), IASPEI (P. Bormann ed.), German Research Centre for Geoscience, Potsdam, Chapter 7, pp. 1-108.

Valensise, G., Pantosti D. (Editors), 2001. The investigation of potential earthquake sources in peninsular Italy: A review, Journal of Seismology, 5, 287-306.

Valoroso L., Chiaraluce L., Piccinini D., Di Stefano R., Schaff D., Waldhauser F., 2013. Radiography of a normal fault system by 64,000 high-precision earthquake locations: The 2009 L'Aquila (central Italy) case study, J. Geophys. Res. Solid Earth, 118, doi:10.1002/jgrb.50130.

Vidale J.E., Shearer P.M., 2006. A survey of 71 earthquake bursts across southern California: exploring the role of pore fluid pressure fluctuations and aseismic slip as drivers. J. Geophys. Res., 111, B05312, doi:10.1029/2005JB004034.

Wessel, P., Smith, W.H.F., Scharroo, R., Luis, J.F., Wobbe, F., 2013. Generic mapping tools: improved version released. Eos. Trans. AGU 94, 409-410. http://dx.doi.org/10.1002/2013EO450001.

Westaway, R., Gawthorpe, R, Tozzi, M., 1989. Seismological and field observations of the 1984 Lazio-Abruzzo earthquakes: implications for the active tectonics of Italy. Geophys. Journal of the Royal Astron. Society, 98, 489-514.

Yang, W., Hauksson, E., 2013. The tectonic crustal stress field and style of faulting along the Pacific North America Plate boundary in southern California, Geophys. J. Int., 194, 100-117.

Tables

Table 1a. Pilot Study temporary seismic stations (October 2009 – January 2010). Digitizer Reftek130, Lennartz 3D 1s sensors, continuous recording mode with 100 sps.

Site station	Latitude	Longitude	Elevation (m)
PF01 – Ridotti	41° 47.72’	13° 36.27’	686
PF02 – Castelliri	41° 42.07’	13° 32.65’	342
PF03 – Casalattico	41° 37.12’	13° 43.28’	562
PF04 – Bisegna	41° 51.99’	13° 46.86’	1376

Table 1b. SLAM temporary seismic stations (November 2011 – December 2013). Digitizer Reftek130, Lennartz 3D/5s sensors, continuous recording mode with 125 sps.

Site station	Latitude	Longitude	Elevation (m)	Sensor
FR01 – Ridotti	41° 47.72’	13° 36.27’	686	Lennartz 3D 5s
FR02 – Casamari	41° 40.32’	13° 29.42’	266	“
FR03 – Casalattico	41° 37.12’	13° 43.28’	562	“
FR04 – Bisegna	41° 51.99’	13° 46.86’	1376	“
FR05 – Ferentino	41° 41.96’	13° 15.78’	387	“
FR06 – Mt. Leuci	41° 27.75’	13° 36.51’	478	“
FR07 – Valvori	41° 33.65’	13° 53.44’	417	“
FR08 – Barrea	41° 44.64’	13° 58.35’	1182	“
FR09 – Rocca d’Evandro	41° 22.65’	13° 55.09’	468	“
FR10 – Sant. della Civita	41° 19.81’	13° 31.24’	642	“
FR11 – Castelnuovo Par.	41° 22.57’	13° 45.89’	465	“
FR12 – Vastogirardi	41° 46.59’	14° 14.58’	1170	“
FR13 – Rifugio Tozze	41° 19.25’	13° 33.64’	795	“
FR14 – Casone Antonucci	41° 47.01’	13° 53.86’	1054	“
FR15 – Pofi	41° 33.76’	13° 26.81’	141	“
FR16 – Chiauci	41° 40.71’	14° 22.72’	941	Lennartz 3D 1s
FR17 – Rendinara	41° 50.16’	13° 28.19’	817	Lennartz 3D 5s
FR18 – Colli di Montebove	42° 05.84’	13° 09.52’	485	“
FR19 – Gallinaro	41° 40.64’	13° 49.22’	484	“
FR20 – Piglio	41° 50.18’	13° 08.30’	856	CMG40
FR21 – Vallecorsa	41° 25.23’	13° 23.39’	326	Lennartz 3D 5s
FR22 – Villa Santa Lucia	41° 25.23’	13° 23.39’	856	“
FR23 – Sezze Scalo	41° 30.16’	13° 02.29’	113	“
FR24 – Valvisciolo	41° 34.05’	13° 58.90’	154	“
FR25 – Radicosa	41° 29.02’	13° 58.14’	671	“
FR26 – San Giovanni Vec. 1	41° 50.13’	13° 32.57’	304	“
FR27 – Sezze montagna	41° 30.85’	13° 01.68’	417	“
FR28 – Fontana Liri	41° 36.62’	13° 33.74’	379	“
FR29 – San Giovanni Vec. 2	41° 50.33’	13° 32.88’	672	“
FR30 – Veroli	41° 44.58’	13° 26.92’	722	“
FR31 – Sora	41° 43.57’	13° 34.11’	397	CMG40
AR04 – Arpino	41° 38.91’	13° 36.59’	460	Lennartz 3D 5s

Table 2. Boundary values of the 1D crustal velocity model; zz depth of the top of each uniform velocity layer.

	V_p	zz
Layer 1	5.40	0.00
Layer 2	5.91	3.50
Layer 3	6.45	7.00
Layer 4	6.65	11.00
Layer 5	5.82	20.01
Layer 6	6.98	31.04

Table 3. Weights assigned to each *P*- and *S*- arrival time on the basis of picking accuracy.

Weights	Picking accuracy (s)
0	0.04
1	0.10
2	0.20
3	0.40
4	1.00

Table 4. Local earthquake dataset of this study (period 2009-2013).

Recording arrays	*P*- picks	*S*- picks	Relocated events	Selected events (quality A + B)	Quality A	Quality B	Rejected events (quality C + D)
RSN, RSA, RSM, SLAM, IESN	60,638	54,565	7011	6270	5803	467	741
Only RSN			4392				

Table 5. Quality factors for fault-plane solution.

Quality	Q_f	Q_p
A	$F_j \leq 0.025$	$\Delta s, \Delta d, \Delta r \leq 20$
B	$0.025 < F_j \leq 0.1$	20 - 40
C	$F_j > 0.1$	> 40

Table 6. Inversions of focal mechanisms for stress tensor orientation.

Sector	σ_1 plunge/trend	σ_2 plunge/trend	σ_3 plunge/trend	R	misfit	Fault plane solut. num.
SW1	86/310	4/125	0/216	0.5	5.1	65
SW2	71/171	18/8	5/276	0.7	3.6	34
SE1	74/139	16/322	1/232	0.5	4.5	39
SW5	12/309	61/62	26/213	0.7	3.0	23

Figure (with caption below and on the same page)

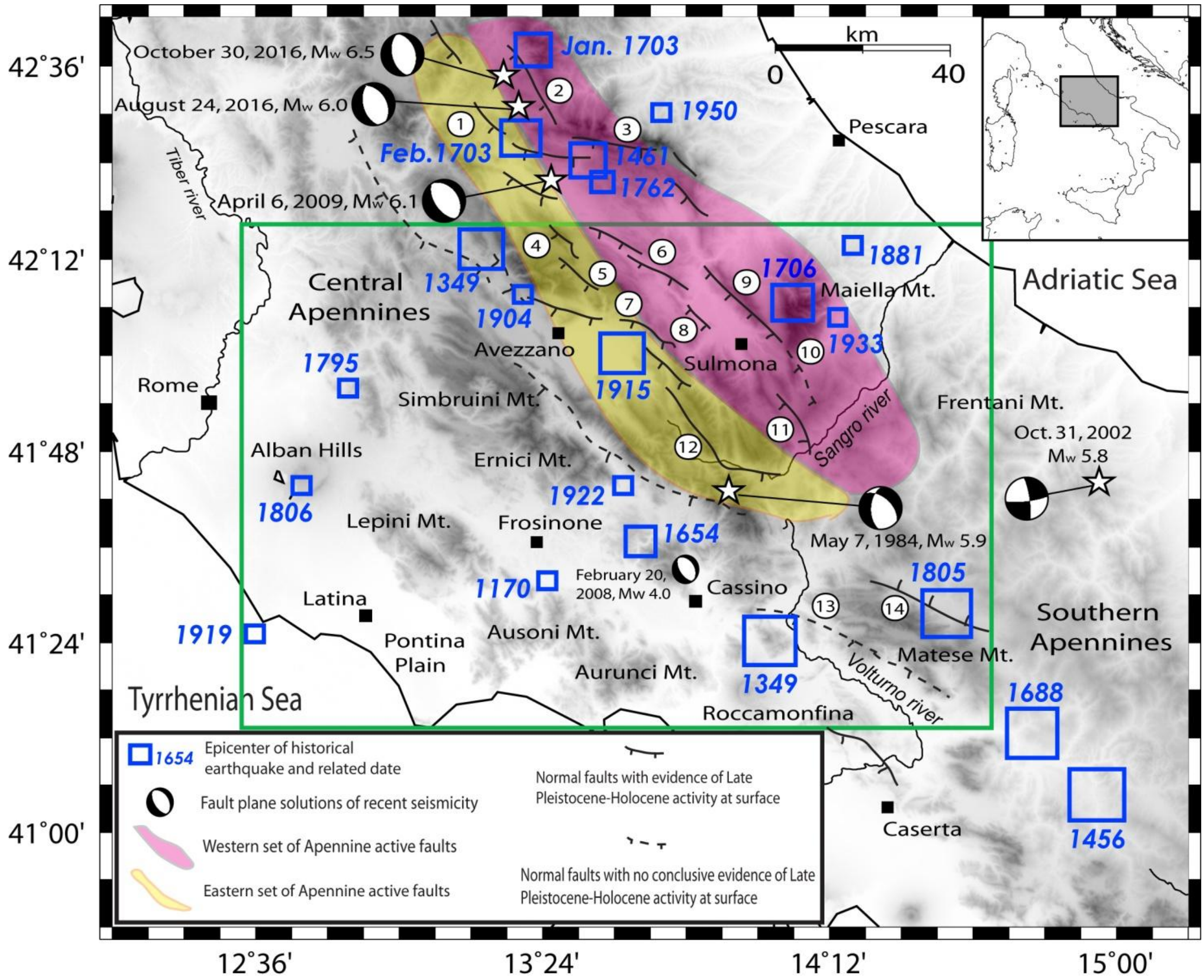

Figure 1. Map with the investigated sector of the central Apennines (green outline). Historical earthquakes after CPTI15 (Rovida et al., 2016), fault plane solutions of recent seismicity and main active faults (modified after Galadini and Galli, 2000): 1) Upper Aterno Valley fault system; 2) Laga Mts. fault; 3) Campo Imperatore fault system; 4) Campo Felice – Colle Cerasitto fault; 5) Ovindoli – Pezza fault; 6) Middle Aterno Valley fault system; 7) Fucino fault; 8) Subequana Valley fault; 9) Morrone Mt. fault; 10) Maiella – Porrara fault system; 11) Aremogna – Cinquemiglia fault; 12) Upper Sangro Valley fault system; 13) Aquae Julia – Venafro fault system; 14) Boiano fault.

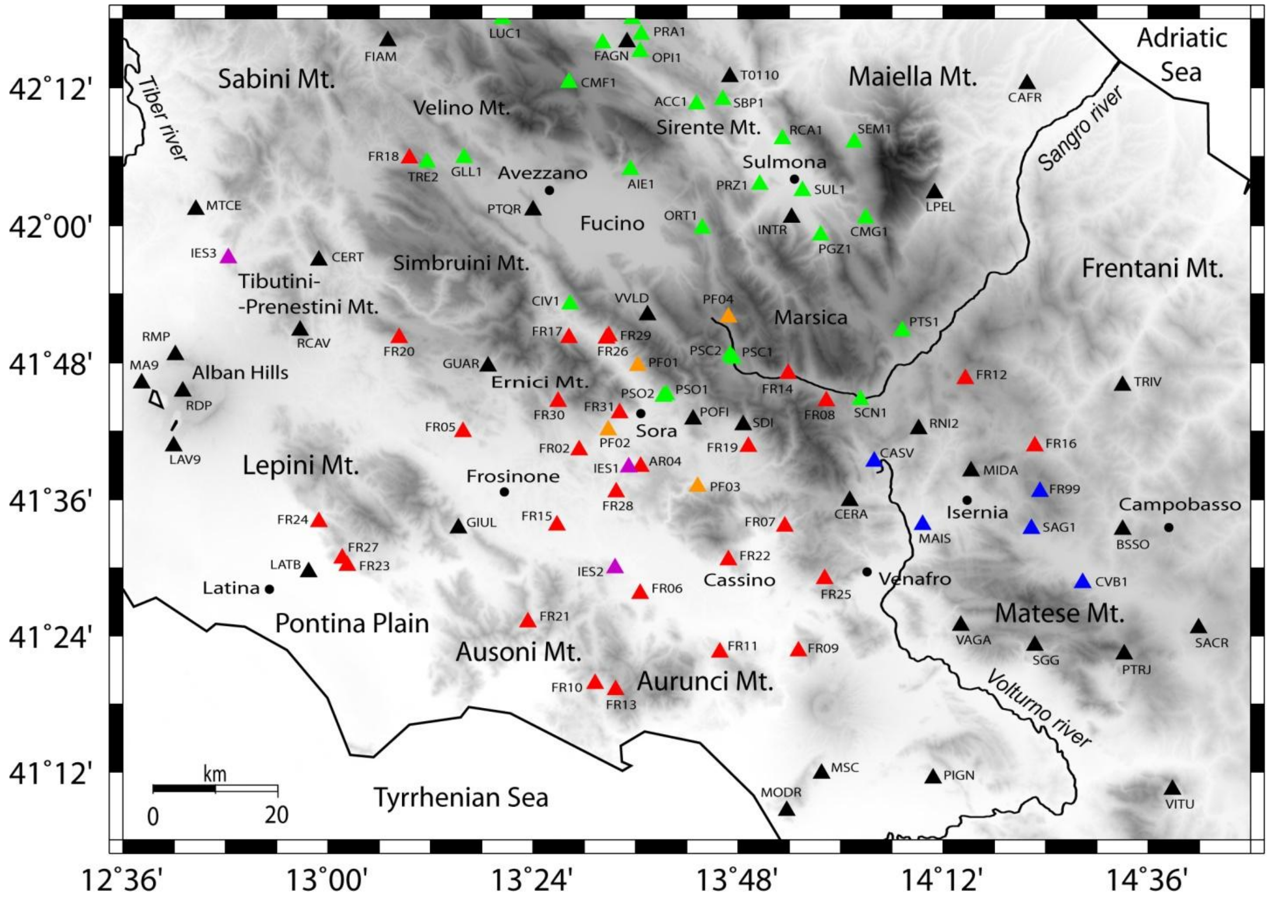

Figure 2. Seismic networks used in this study; a) National Seismic Network (RSN, black triangles); b) Abruzzo Regional Seismic Network (RSA, green); c) Molise Regional Seismic Network (RSM, dark blue); d) pilot temporary network (2009-2010) (orange); e) SLAM project temporary network (2011-2013) (red); f) Italian Earthquake Seismic Network (IESN) (purple).

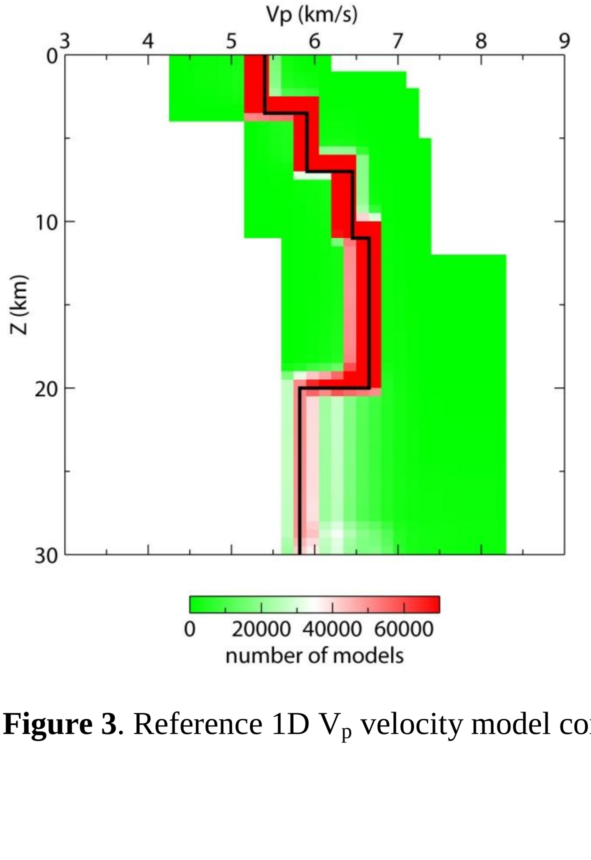

Figure 3. Reference 1D V_p velocity model computed by the application of a genetic algorithm.

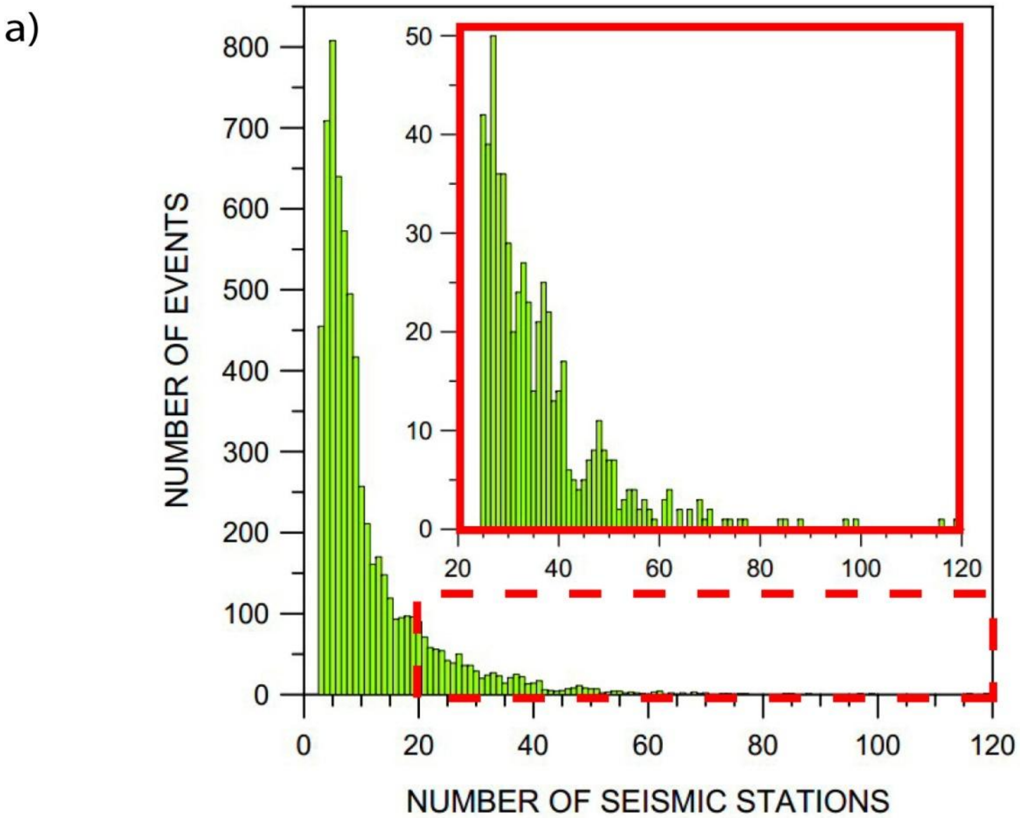

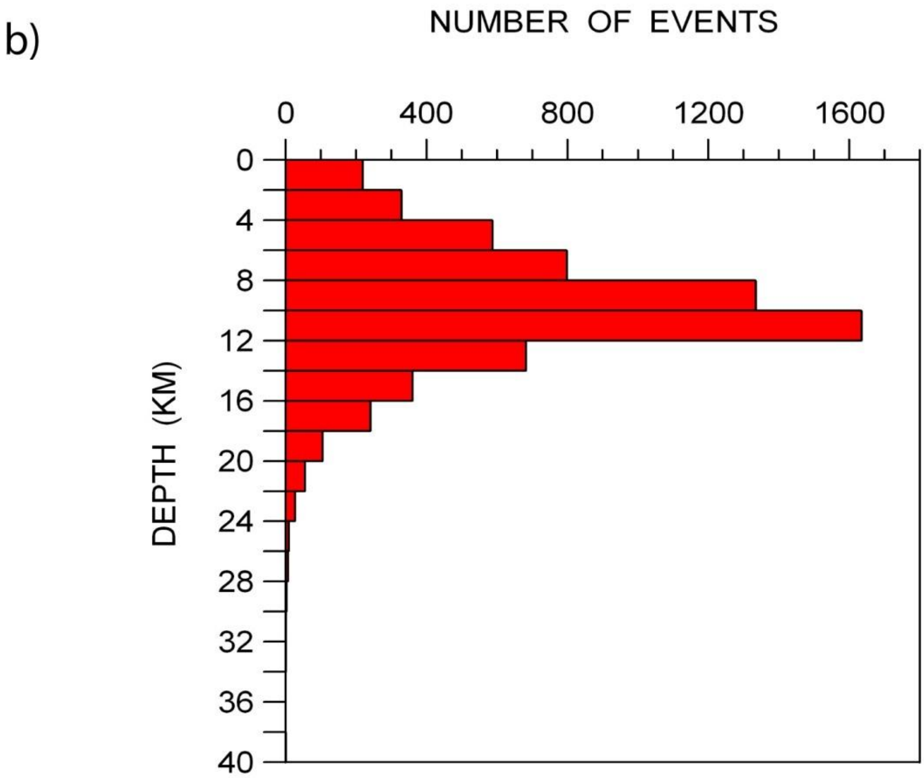

Figure 4. a) Number of events for each recording station and b) distribution with depth.

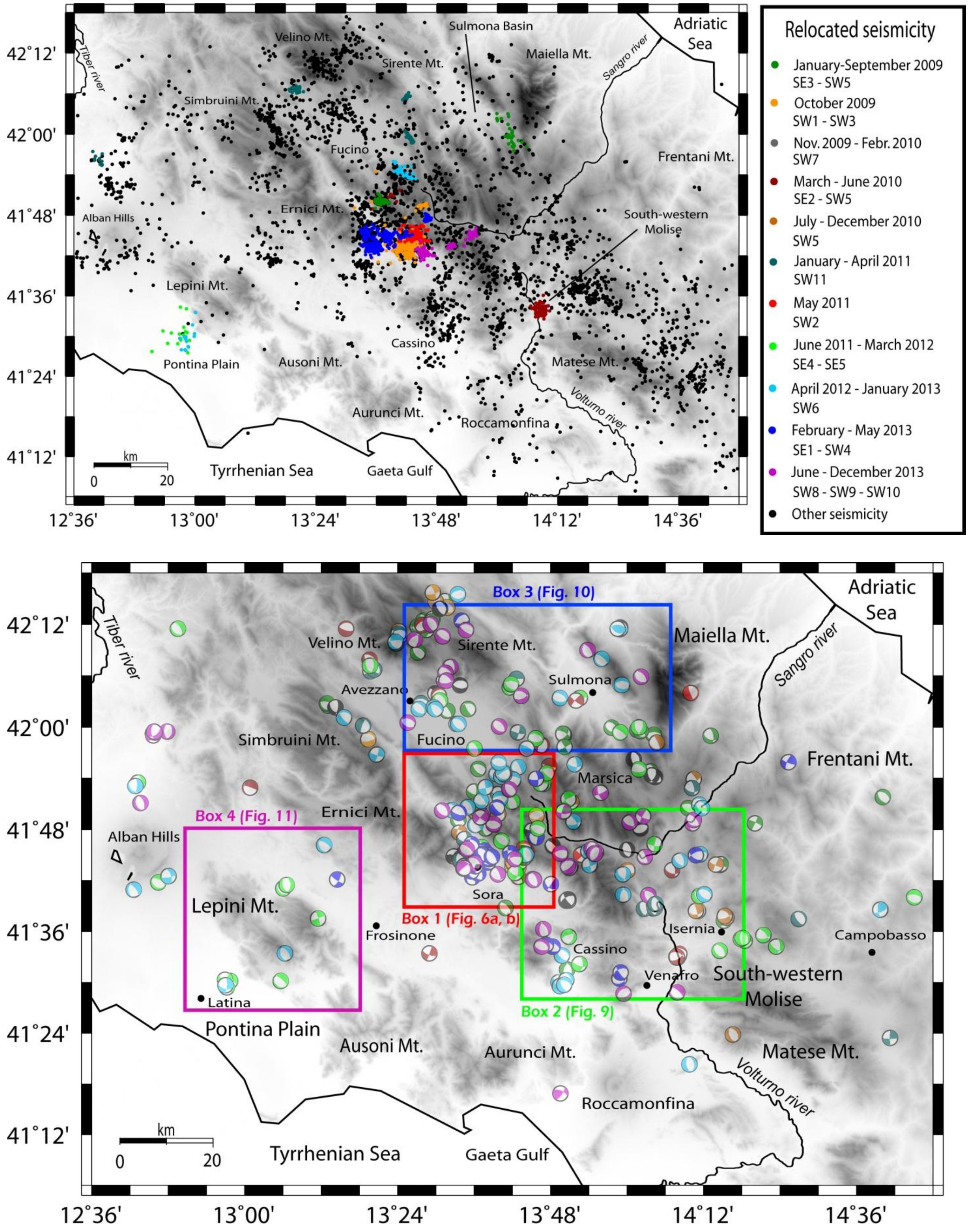

Figure 5. a) Epicentral location of the 6270 earthquakes selected for the analysis. Coloured dots indicate the major swarms and sequences recognized during our observing period (see legend on the right). b) Map with the 468 focal mechanisms computed in this work. Coloured boxes (from 1 to 4) indicate the areas shown in Figures 6a,b and 9-11.

Box 1

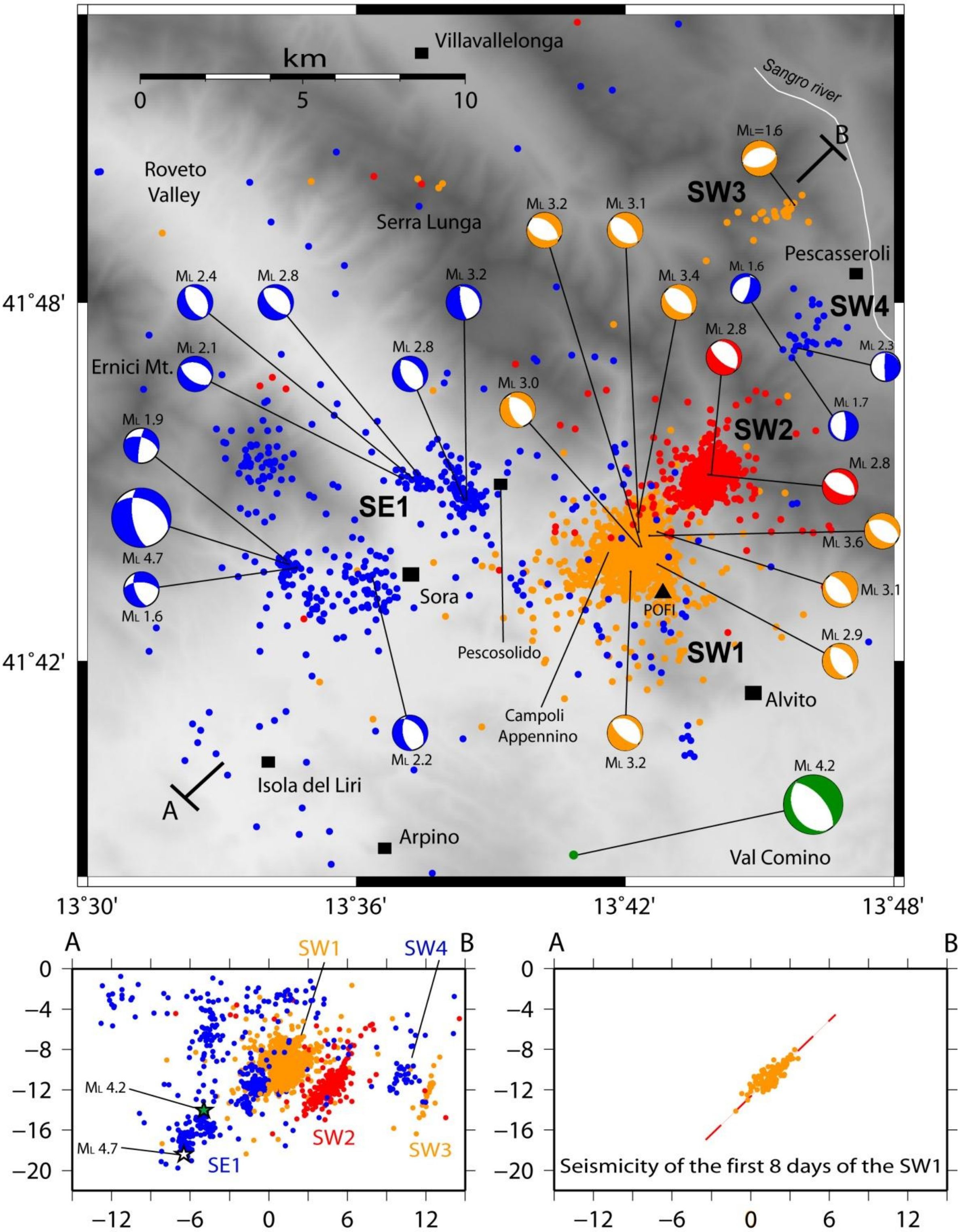

Villavallelonga
km
0 5 10
Sangro river
Roveto Valley
Serra Lunga
SW3
Pescasseroli
SW4
Ernici Mt.
SE1
SW2
Sora
Pescosolido
POFI
SW1
Campoli Appennino
Alvito
Isola del Liri
Arpino
Val Comino
A
B
41°48'
41°42'
13°30'
13°36'
13°42'
13°48'
ML 4.7
ML 4.2
SW1
SW4
SW2
SW3
SE1
Seismicity of the first 8 days of the SW1

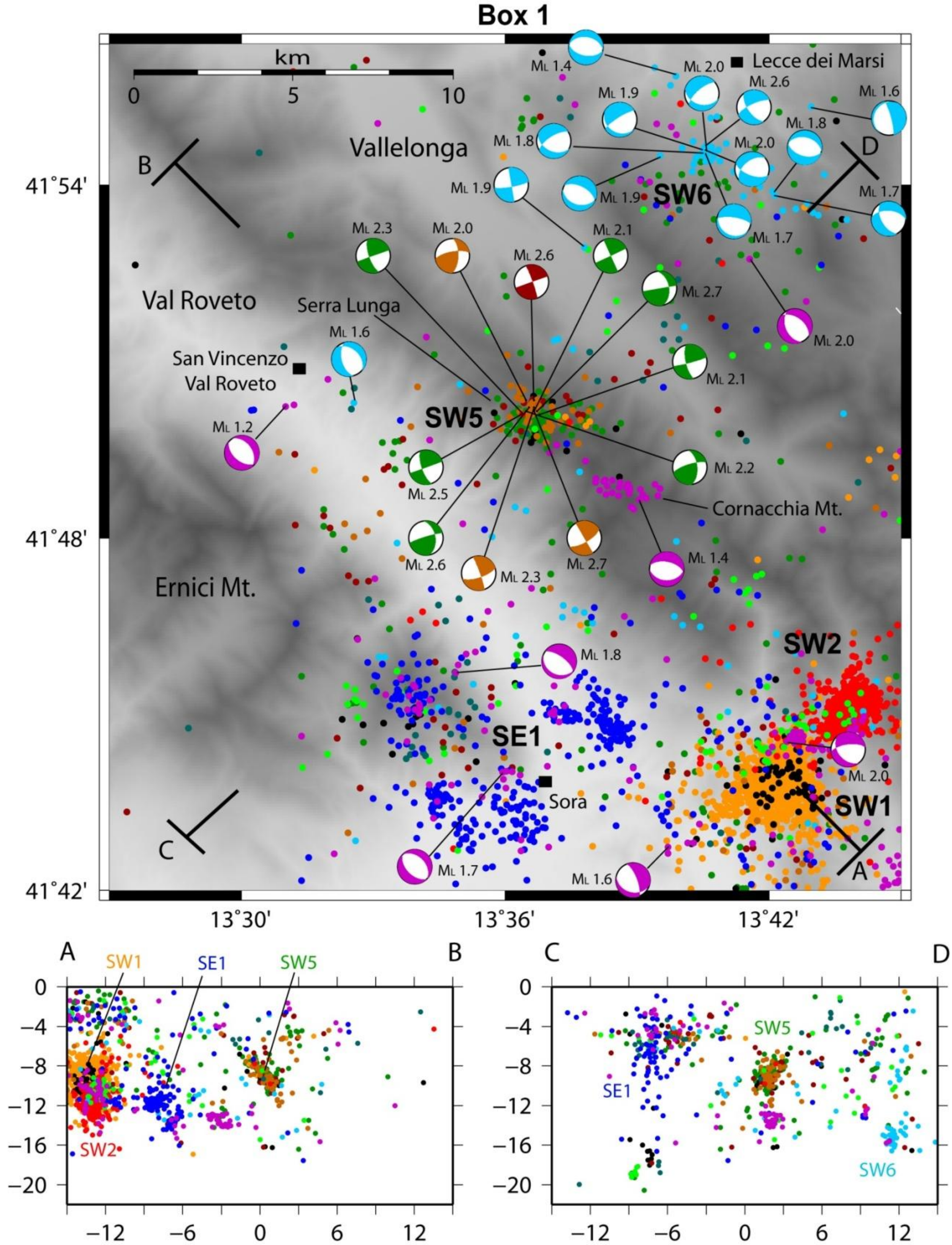

Figure 6. a) Map of the MSA with the location of the M_L 4.2 earthquake (August 6, 2009, dark green), the SW1 and SW2 swarms (October 2009 in orange, May 2011 in red) and the SE1 sequence (February-March 2013 in blue). White star in the cross-section shows the epicentre of the main shock of the 2013 Sora sequence (M_L 4.7) and the green one that of the M_L 4.2 earthquake. Orange dots in the cross-section on the right side represent events only of the first 8 days of the SW1. They delineated a very clear seismic structure dipping to the SW. In this map, the remaining part of the study seismicity is omitted for sake of simplicity. b) Map of the Val Roveto and Vallelonga area with the Serra Lunga cluster (SW5, dark green, dark red and brown dots, April 2009-December 2010). The Lecce dei Marsi swarm (SW6, pale blue dots, October-December 2012) is also shown.

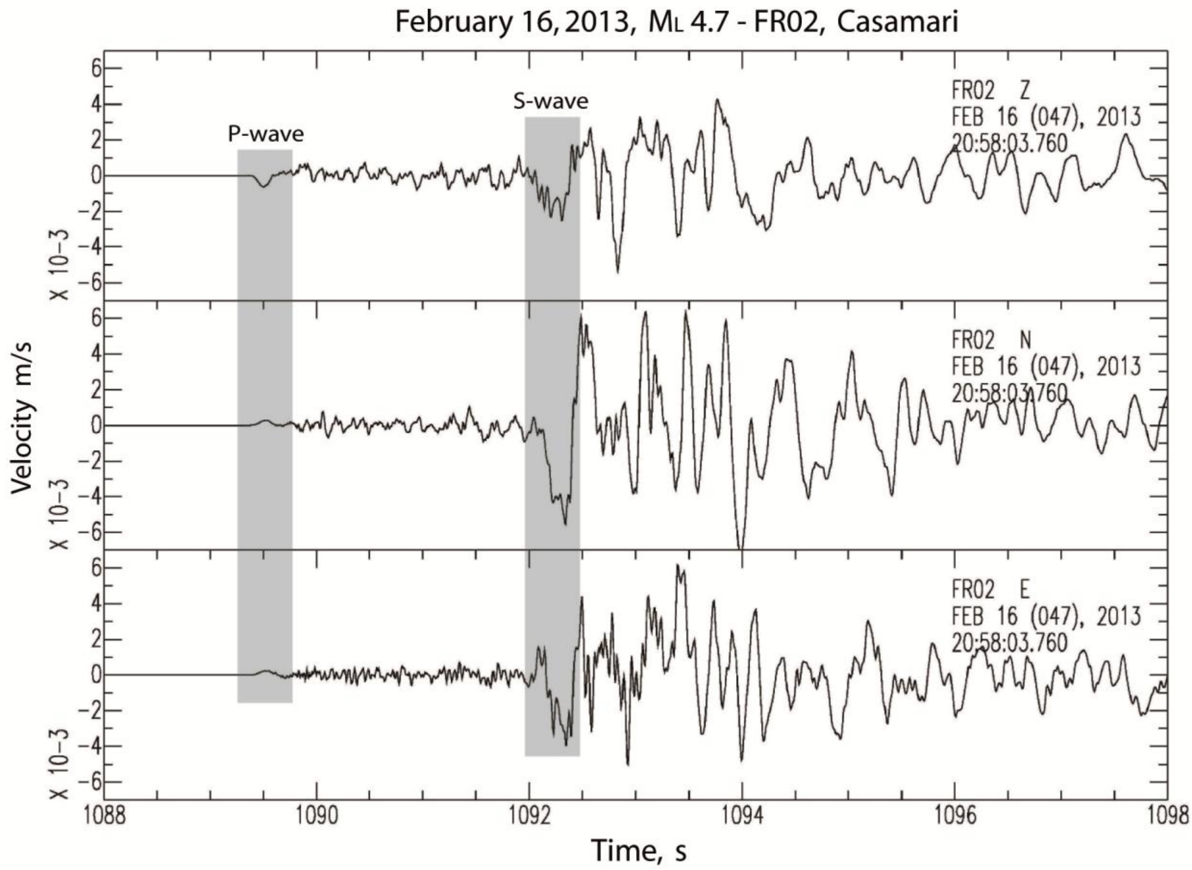

Figure 7. Three component seismograms of the February 16, 2013 M_L 4.7 Sora main shock recorded at the closest station of the SLAM array, station FR02 (Casamari). It was located about 10 km from the epicentre in the SW direction.

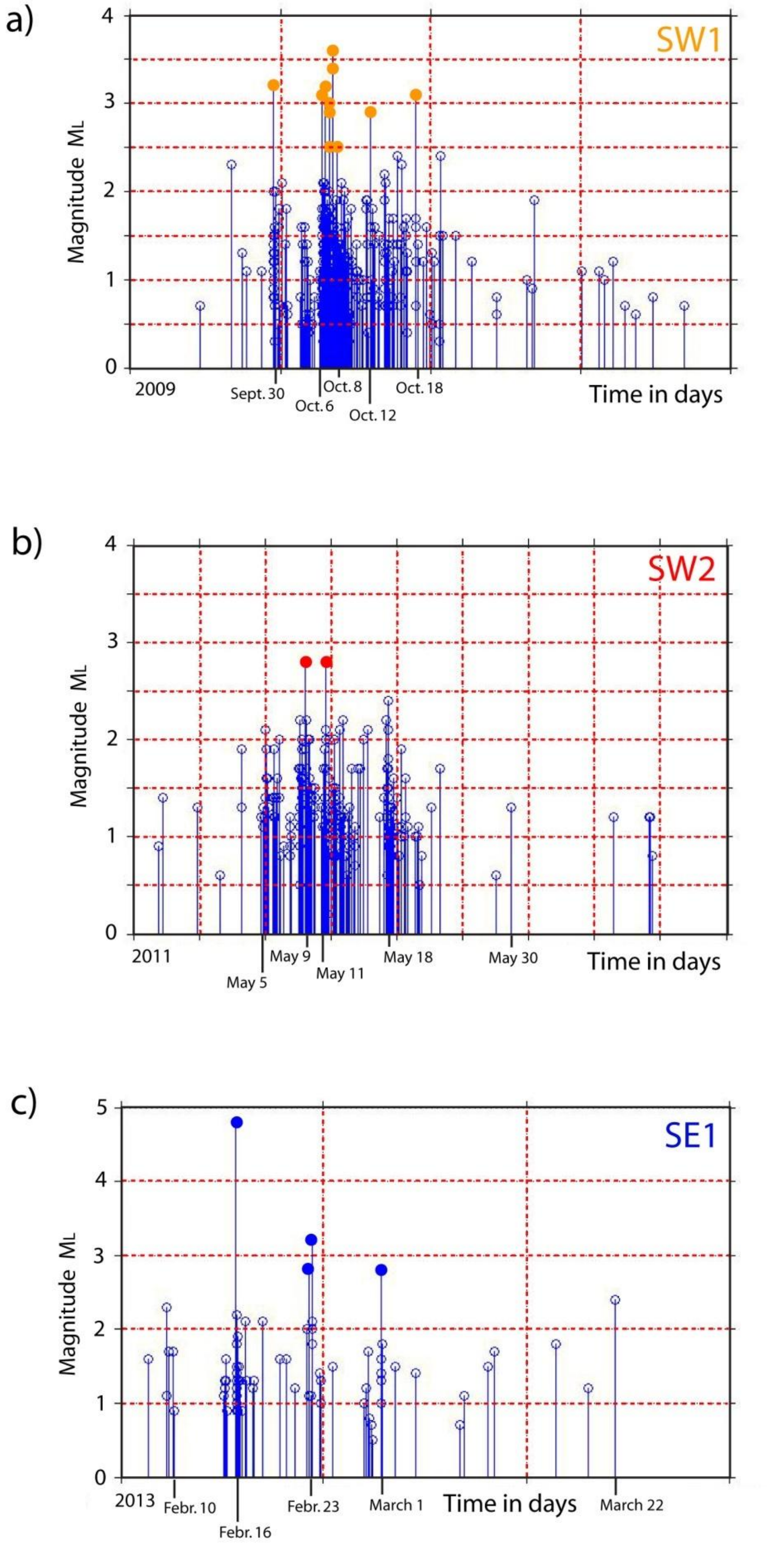

Figure 8. Magnitude time evolution plots of the MSA seismcity: a) SW1 (October 2009); b) SW2 (May 2011); c) SE1 (February-March 2013). Coloured dots show larger magnitude events.

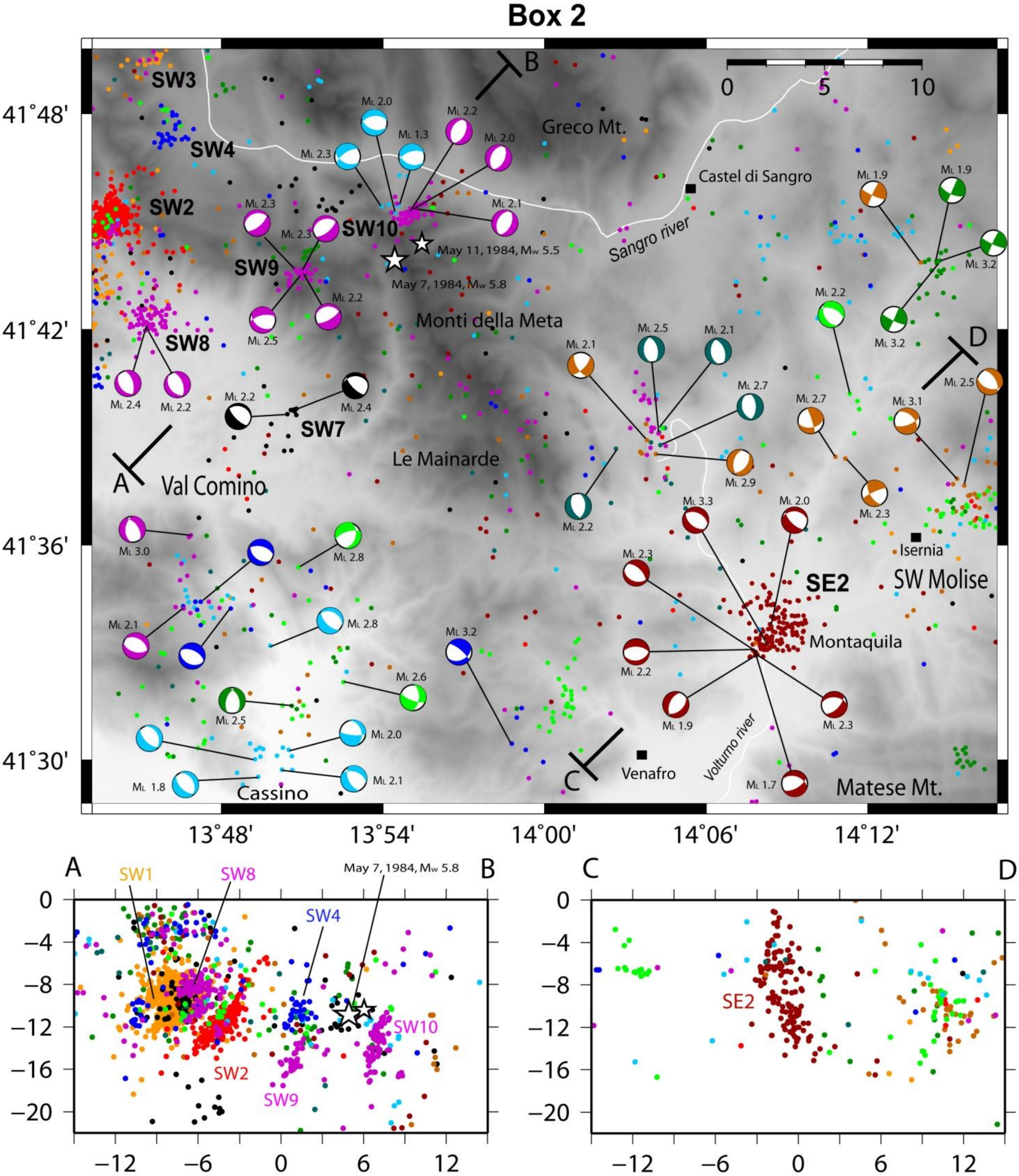

Figure 9. Map of the Val Comino and south-western Molise areas. In black the small seismic swarm of Settefrati (SW7, November 2009). In purple the three seismic swarms of June-August 2013 (SW8, SW9 and SW10). White stars show the epicentres of the two main shocks of the 1984 Val Comino sequence. In dark red is shown the Montaquila sequence (SE2, May 2010). Events with right lateral strike-slip solutions (dark green and brown fault plane solutions) are located in the NE part of this sector.

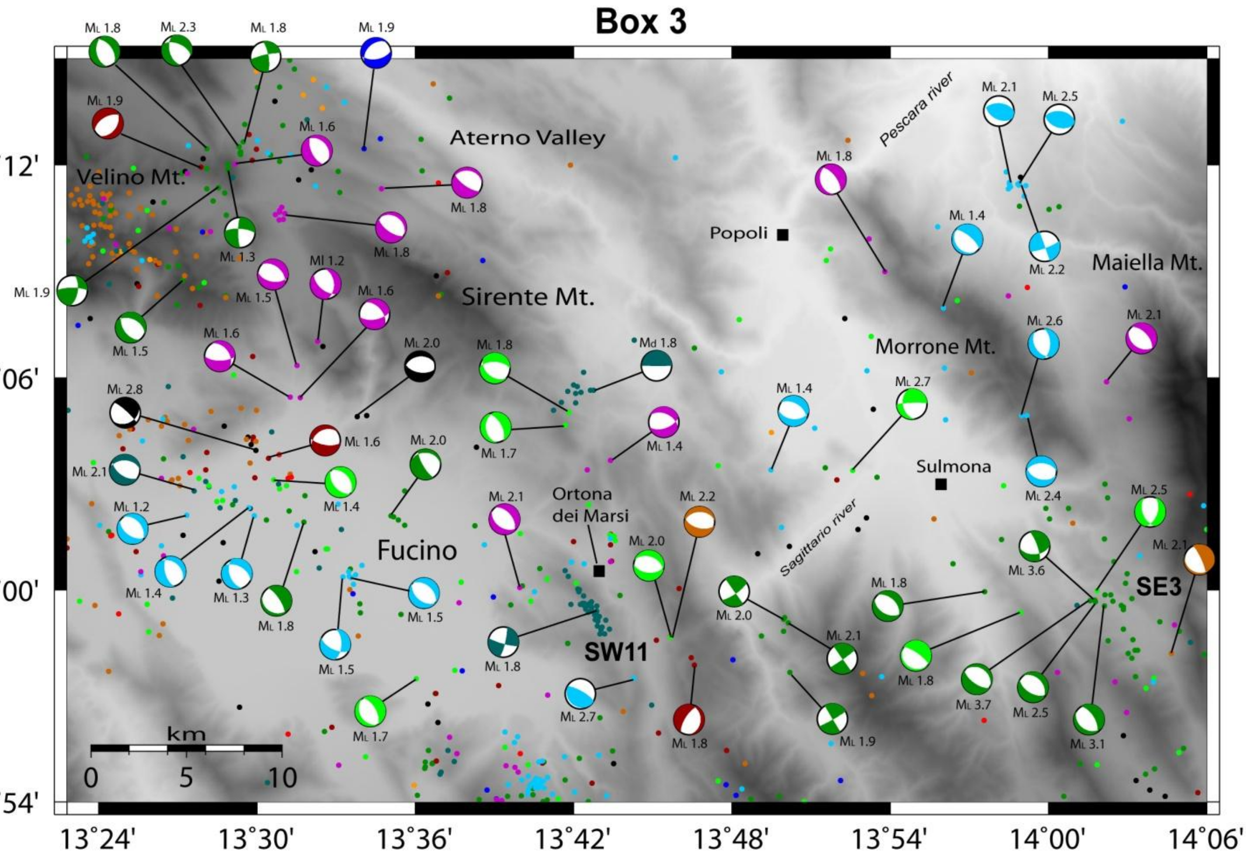

Figure 10. Map of the Sulmona basin, Fucino and Velino-Sirente Mts. areas. The small sequence (SE3, dark green dots) that started before the April 6, 2009 L'Aquila earthquake, in March 17, with a magnitude M_L 3.6 event, is shown. A small swarm occurred near Ortona dei Marsi (March-April 2011) along a NW-SE direction (SW11, green-grey dots). The only reliable focal mechanism of this swarm shows a strike-slip solution.

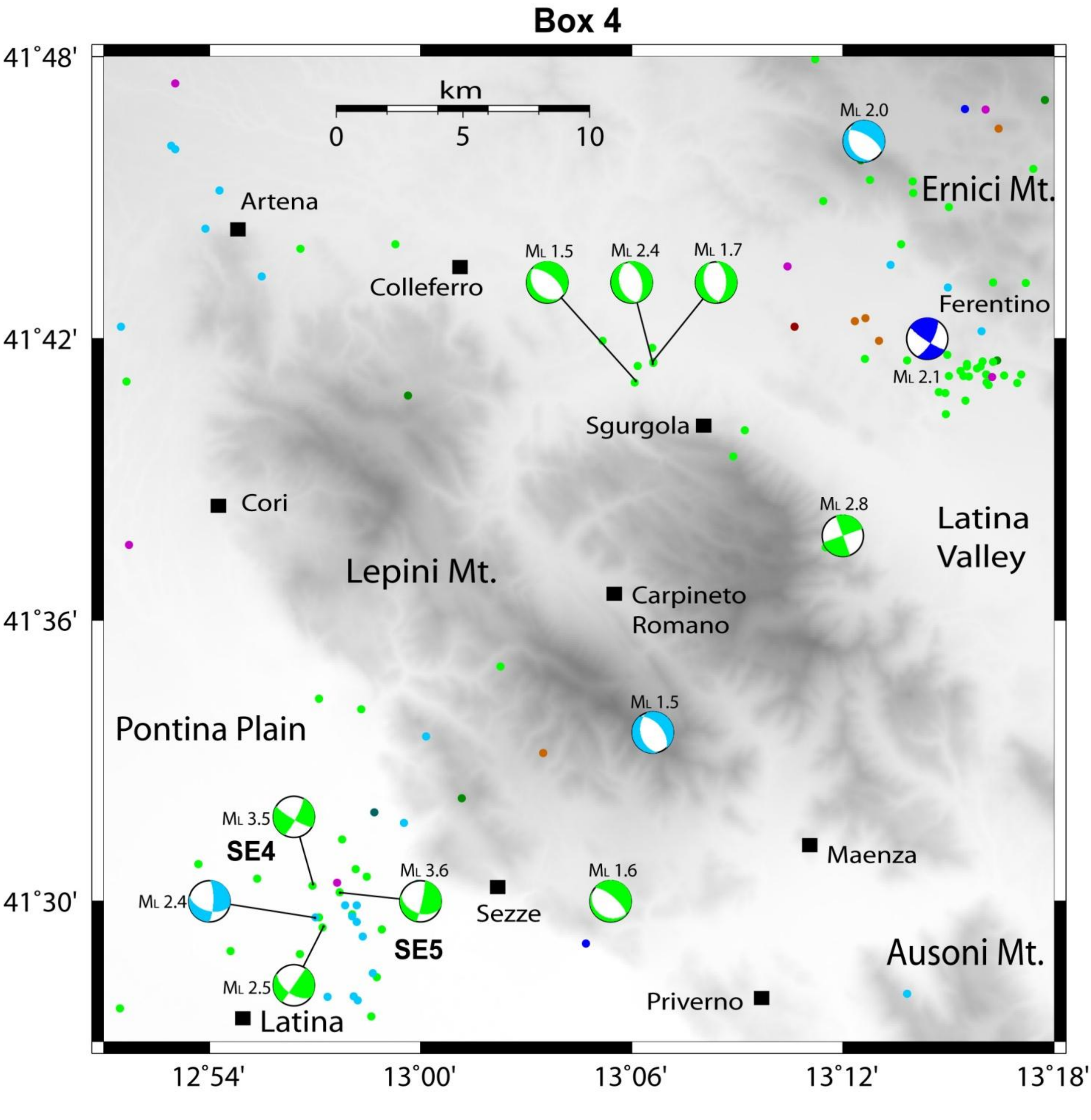

Figure 11. Map with the seismicity of the Pontina Plain (Latina sequences 2011 and 2012, SE4 and SE5, green and pale blue dots) and Lepini Mountains.

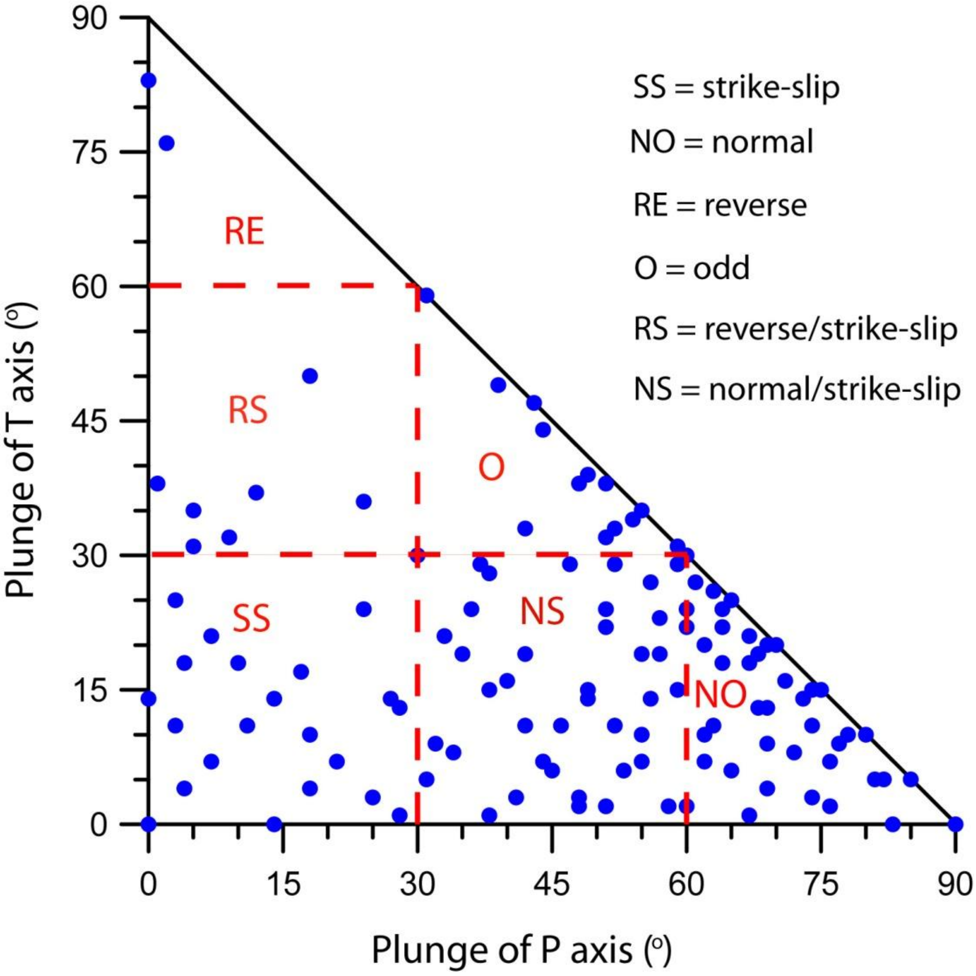

Figure 12. Dip angle of T-axes vs. dip angle of P-axes for the 468 fault plane solutions of this study. In this diagram the vertices represent strike-slip (SS), reverse (RE) and normal (NO) solutions. RS and NS are oblique-type mechanisms whereas the solutions in the field O are defined as odd. Note the predominance of SS, NS and NO solutions.

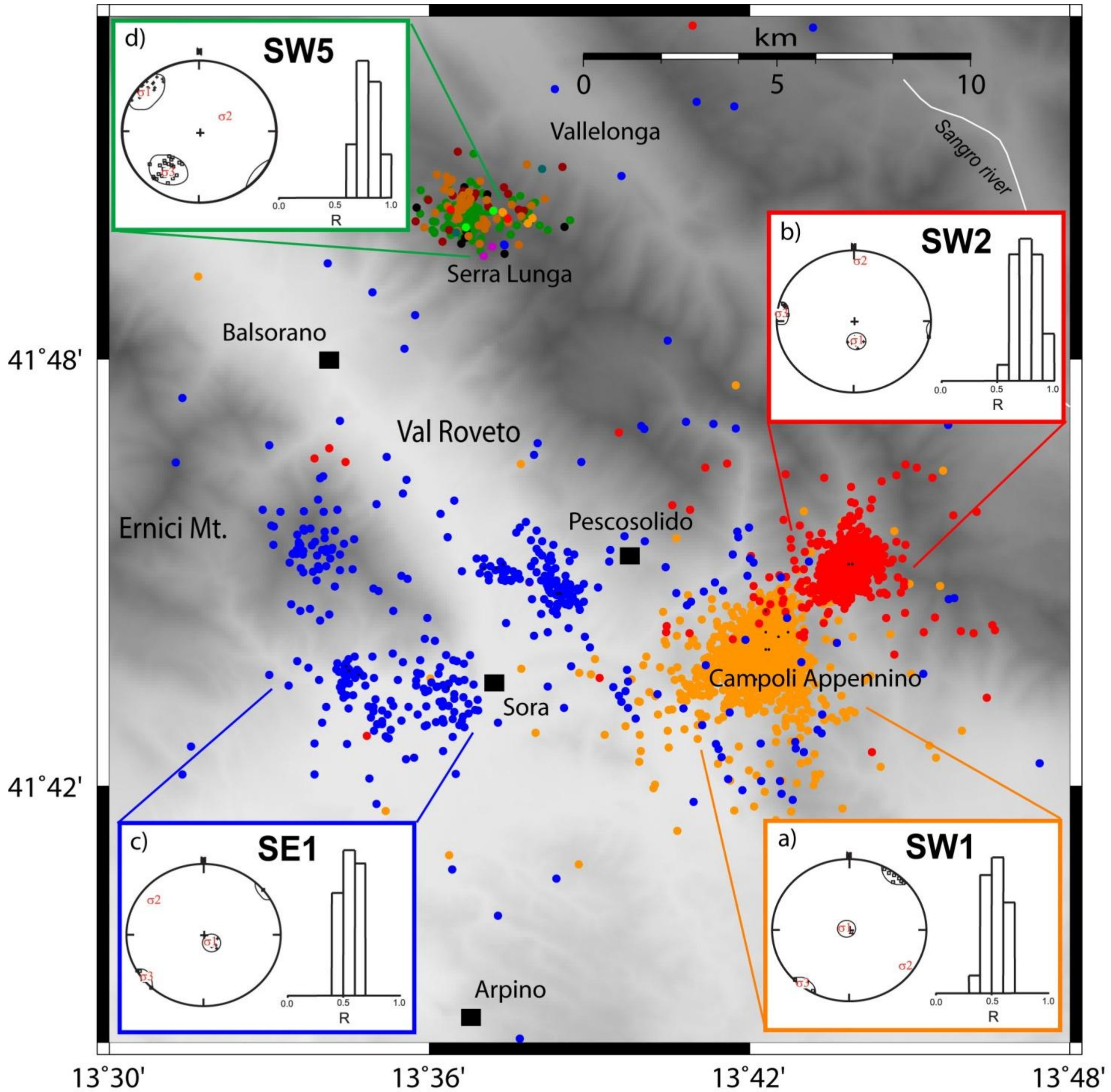

Figure 13. Stress inversion results for the MSA (a) using 65 fault plane solutions of the SW1 (October 2009); (b) 34 solutions of the SW2 (May 2011); (c) 39 solutions of the SE1 (February-March 2013); (d) 23 solutions of the SW5 (2009-2010). For each inversion we show the stereonet plot with 95% confidence limits for σ_1 (small crosses) and σ_3 (small squares) and the histogram illustrating the uncertainty in the stress ratio R. Plunge and trend values for the three principal stress axes with the R parameter and the misfit are listed in Table 6.